Plasma instability and amplification of electromagnetic waves in low-dimensional electron systems

S. A. Mikhailov*
Max-Planck Institut für Physik komplexer Systeme, Nöthnitzer Strasse 38, D-01187 Dresden, Germany
(Received 19 December 1997)

Twenty years ago active experimental studies of plasma oscillations in two-dimensional electron systems (2DES's) in Si metal-oxide-semiconductor field-effect transistors and GaAs/$Al_xGa_{1-x}As$ heterostructures began. From the outset the idea of using the radiative decay of grating-coupled 2D plasmons for creation of tunable solid-state far-infrared sources has been discussed in the literature; however, numerous attempts to realize it in far-infrared 2D plasmon emission experiments (in which the plasmons are excited by a strong dc current flowing in the 2DES) have failed: the intensity of radiation turned out to be too small to be promising for device applications. We present a complete analytic theory of a grating-coupled 2DES with a flowing current. We show why the devices have not worked properly so far, and what should be done to increase the radiation, to get an amplification of light, and to reduce threshold currents of amplification down to experimentally achievable values. The main idea of the work—to replace the commonly employed *metal* grating by a *quantum-wire* one—allows one essentially to reduce threshold currents, and to increase the amplification of waves by several orders of magnitude. We show that tunable far-infrared emitters, amplifiers, and generators can be created at realistic parameters of modern semiconductor heterostructures. This work opens new ways to the practical implementation of plasma waves in low-dimensional electron systems. [S0163-1829(98)01127-8]

I. INTRODUCTION

The motion of a fast electron beam across a periodic metal structure results in the radiation of electromagnetic waves. This phenomenon, often referred to as the Smith-Purcell effect,[1] provides the basis for a number of vacuum devices, such as traveling wave tubes and backward wave tubes. In these devices electrons accelerated by an applied electric field up to a velocity v_{dr} move in vacuum across a periodic metal structure (a grating or a spiral), which leads to an amplification or generation of electromagnetic waves at the frequency $f \sim v_{dr}/a$, where a is the grating period. The drift velocity v_{dr} here is determined by the applied electric voltage, so that these devices are *voltage tunable* amplifiers and generators.

The vacuum devices successfully operate in the radio and microwave range. A further enhancement of the operating frequency presents severe difficulties because of the mechanical instability of a freely standing in vacuum periodic structure of metal wires with a very small period. The operating frequency of vacuum devices cannot therefore be extended up to the far-infrared (FIR) range.

In the late 1970s active experimental research of plasma oscillations in two-dimensional (2D) electron systems (ES's) in Si metal-oxide-semiconductor field-effect transistors (MOSFET's) and GaAs/$Al_xGa_{1-x}As$ heterostructures began.[2–5] In a considerable part of the experimental work (for a review see Ref. 6) FIR *transmission* spectroscopy has been used for the detection of 2D plasmons (Fig. 1, where $v_{dr}=0$). In this technique, the 2D plasmons, which are normally nonradiative modes,[7] are coupled to electromagnetic radiation by a metal grating placed in the vicinity of the 2D layer. An incident electromagnetic wave with the intensity I_0 and the electric field polarized perpendicular to the grating strips passes through the structure in the direction perpendicular to the 2D layer (z direction), and the spectrum of the transmitted wave $T(\omega)$ is registered. Well-defined resonances that correspond to an excitation of 2D plasmons with reciprocal lattice vectors $\mathbf{G}_m=(2\pi m/a,0)$ are observed in the transmission spectrum (here a is the grating period and m is integer). In experiments of this type the energy of the external electromagnetic wave is converted to the energy of the 2D plasmons.

Figure 1 resembles the geometry of the tunable vacuum amplifiers and generators: the system consists in a conducting electron (2D) layer where electrons can move under the action of an applied electric field, and an adjacent grating. The first attempts to observe the emission of light from the grating-coupled 2DES were made, to the best of our knowl-

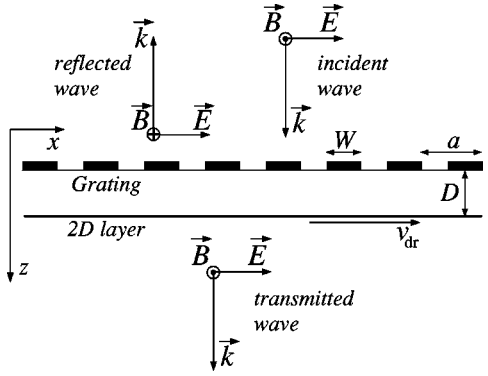

FIG. 1. The geometry of the considered structure. The system is infinite in the y direction. 2D electrons are moving in the x direction perpendicular to the grating strips with the drift velocity v_{dr}. A transmission spectroscopy experiment corresponds to $v_{dr}=0$, $I_0 \neq 0$, an emission spectroscopy experiment corresponds to $v_{dr}\neq 0$, $I_0=0$, where I_0 is the intensity of the incident wave.

 © 1998 The American Physical Society

edge, in 1980.[8,9] In these FIR *emission* experiments (Fig. 1, where the drift velocity $v_{dr} \neq 0$, but the intensity of the incident light I_0 is zero) a strong dc current is passed through the 2D layer (in the x direction perpendicular to the grating strips), and the emitted electromagnetic radiation is registered. The grating period in these solid-state structures can be made smaller than 1 μm, and the typical frequency of 2D plasmons falls in the terahertz (FIR) range. A successful realization of the 2D plasmon emission experiment could lead to a creation of a tunable solid-state source of the FIR electromagnetic radiation. In spite of the strong appeal of this idea and a number of more recent experiments,[10–13] the intensity of radiation from the 2DES remains very small, and successfully working solid-state devices based on the discussed principle are absent so far.

The energy of the dc current passing through an electron system in the presence of the grating is converted to electromagnetic radiation in two steps. First, it is transformed to the energy of plasma oscillations in the beam by means of a current-driven plasma instability.[14,15] Then the energy stored in the plasmon field is converted to electromagnetic radiation by means of the grating. The plasma instability develops in the system when the drift velocity of electrons exceeds a threshold value v_{th}, estimated as the plasma frequency of electrons in the beam divided by a typical grating wave vector $G_1 = 2\pi/a$ [see Eq. (55) below, as well as Ref. 15]. In vacuum devices the plasma frequency in the electron beam is much smaller than that in the 2DES, and electrons can be accelerated up to velocities much higher than those achievable in solid-state structures. The threshold condition for amplification is thus more difficult to satisfy in solid-state structures than in their vacuum counterparts, therefore the first attempts to realize the emission of light from the grating-coupled 2DES have failed.

The aim of this paper is to develop a general theory of the transmission, amplification, and emission of light in the structure ''grating coupler–2DES,'' and to find realistic ways to reduce the threshold velocity of amplification. We consider a propagation of light through the structure ''grating coupler–2DES *with a flowing current*'' (Fig. 1 with $v_{dr} \neq 0$ and $I_0 \neq 0$), and calculate the transmission $T(\omega, v_{dr})$, reflection $R(\omega, v_{dr})$, absorption $A(\omega, v_{dr})$, and emission $E(\omega, v_{dr})$ (at $I_0 = 0$) coefficients as a function of the light frequency ω, the drift velocity v_{dr}, and other physical and geometrical parameters of the system. In the literature the problem of the transmission of light ($v_{dr} = 0$, $I_0 \neq 0$) has been solved analytically in a *perturbative* approach[16,6] (the grating has been treated as an infinitely thin metal layer with a weakly modulated density), and numerically in a nonperturbative approach.[17] An emission of light from the structure ''metal grating–2DES'' ($v_{dr} \neq 0$, $I_0 = 0$) has been considered by Kempa *et al.*[18] using a numerical nonperturbative approach. We solve the problem *analytically* using the *nonperturbative* technique recently proposed in Refs. 19–21. One of the main results of our work is that the amplification of waves can be drastically increased, and the threshold velocity can be essentially reduced (down to experimentally achievable values) in structures ''2DES–*quantum-wire* grating'' (contrary to commonly employed structures with *metal* gratings). The effect is due to the resonant interaction of 2D plasmons with plasmons of the grating, which leads to a remarkable enhancement of the grating coupler efficiency, and finally to an improvement of device characteristics.

The paper is organized as follows. In Sec. II we develop a general theory of the scattering of electromagnetic waves on the structure ''grating coupler–thin conducting layer.'' In Sec. III we apply the general formalism to an analysis of the FIR transmission, reflection, and absorption spectra of the grating-coupled 2DES without the dc electric current. In Sec. IV we study an amplification of FIR radiation passing through the system with a flowing current. In Sec. V we discuss an emission spectrum of the structure ($v_{dr} \neq 0$, $I_0 = 0$) and compare our approach with that of Ref. 18. In Sec. VI we summarize our results and formulate particular recommendations for a designing tunable solid-state FIR amplifiers.

II. SCATTERING OF LIGHT ON A GRATING-COUPLED THIN CONDUCTING LAYER: GENERAL THEORY

In this section we develop a general theory of the scattering of light on a structure ''grating coupler–thin conducting layer'' (Fig. 1). The grating coupler is treated as an infinitely thin[22] conducting layer with an electron density

$$N_1(x)\,\delta(z) = \sum_k n_1(x - ak)\,\delta(z), \tag{1}$$

placed in the plane $z = 0$. The continuous function $n_1(x)$ is assumed to be zero at $|x| > W/2$ and an arbitrary nonzero function at $|x| < W/2$, where W is the width of the grating strips and a is the grating period. The conducting layer (2DES) is placed in the plane $z = D$ and described by the frequency and wave-vector-dependent conductivity $\sigma_{2D}(\mathbf{q}, \omega)$ [all quantities related to the grating (2DES) will be supplied by the index 1 or 1D (2 or 2D)]. The electromagnetic wave is assumed to be incident upon the structure along the z axis with the electric vector polarized in the x direction, perpendicular to the grating strips. The system is infinite in the y direction, and a background dielectric constant ϵ is uniform in all the space.

The total electric field $\mathbf{E}^{tot}$ satisfies the Maxwell equations,

$$\nabla \times (\nabla \times \mathbf{E}^{tot}) + \frac{\epsilon}{c^2} \frac{\partial^2 \mathbf{E}^{tot}}{\partial t^2} = -\frac{4\pi}{c^2} \frac{\partial}{\partial t} [\mathbf{j}^{1D}(x)\,\delta(z) + \mathbf{j}^{2D}(x)\,\delta(z - D)], \tag{2}$$

with scattering boundary conditions at $z \to \pm\infty$. We search for a solution in the form

$$\mathbf{E}^{tot}(\mathbf{r}, z) = \sum_{\mathbf{G}} [\mathbf{E}^{ext}_{\mathbf{G}}(z) + \mathbf{E}^{ind}_{\mathbf{G}}(z)] e^{i\mathbf{G}\cdot\mathbf{r} - i\omega t}, \tag{3}$$

where $\mathbf{G} = \mathbf{G}_m = (2\pi m/a, 0)$, and the incident (external) and the scattered (induced) electromagnetic waves are written as

$$\mathbf{E}^{ext}_{\mathbf{G}}(z) = \begin{pmatrix} E^{ext}_{x,\mathbf{G}} \\ 0 \\ 0 \end{pmatrix} e^{i\omega\sqrt{\epsilon}z/c}, \quad E^{ext}_{x,\mathbf{G}} = E_0\,\delta_{\mathbf{G},\mathbf{0}}, \tag{4}$$

and $\mathbf{E}_{\mathbf{G}}^{\rm ind}(z)=[E_{x,\mathbf{G}}^{\rm ind}(z),0,E_{z,\mathbf{G}}^{\rm ind}(z)]$. The field $E_{x,\mathbf{G}}^{\rm ind}(z)$ satisfies the equation

$$\frac{\partial^2 E_{x,\mathbf{G}}^{\rm ind}}{\partial z^2}-\kappa_{\mathbf{G}}^2 E_{x,\mathbf{G}}^{\rm ind}=\frac{4\pi i\kappa_{\mathbf{G}}^2}{\omega\epsilon}[j_{x,\mathbf{G}}^{\rm 1D}\delta(z)+j_{x,\mathbf{G}}^{\rm 2D}\delta(z-D)], \tag{5}$$

and has a solution

$$E_{x,\mathbf{G}}^{\rm ind}(z)|_{z<0}=A_{\mathbf{G}}\exp(\kappa_G z), \tag{6a}$$

$$E_{x,\mathbf{G}}^{\rm ind}(z)|_{0<z<D}=B_{\mathbf{G}}\sinh(\kappa_G z)+C_{\mathbf{G}}\cosh(\kappa_G z), \tag{6b}$$

$$E_{x,\mathbf{G}}^{\rm ind}(z)|_{z>D}=D_{\mathbf{G}}\exp(-\kappa_G z), \tag{6c}$$

where

$$\kappa_{\mathbf{G}}\equiv\kappa_G=\sqrt{G^2-\omega^2\epsilon/c^2}. \tag{7}$$

If $G_m=2\pi m/a=0$, the value $\kappa_{G=0}=-i\omega\sqrt{\epsilon}/c$ is imaginary (the radiative boundary conditions at $z\to\pm\infty$ imply that Im $\kappa_G<0$), and the values $A_{\mathbf{G}=\mathbf{0}}$ and $E_0+D_{\mathbf{G}=\mathbf{0}}$ give the amplitudes of *normally* reflected and transmitted waves. If κ_G is imaginary for several nonzero m (i.e., at $\omega\sqrt{\epsilon}/c>G_m$), the values $A_{\mathbf{G}}$ and $D_{\mathbf{G}}$ describe the amplitudes of reflected and transmitted waves in corresponding (mth) diffraction orders. For all $|m|>a/\lambda$, where $\lambda=2\pi c/\omega\sqrt{\epsilon}$ is the wavelength of light, $A_{\mathbf{G}}$ and $D_{\mathbf{G}}$ give the amplitudes of evanescent (nonpropagating) electric field.

Using boundary conditions at the planes $z=0$ and $z=D$ we relate the amplitudes of the electric field $A_{\mathbf{G}},\ldots,D_{\mathbf{G}}$ to the Fourier components of the electric current:

$$A_{\mathbf{G}}=C_{\mathbf{G}}=-\frac{2\pi i\kappa_G}{\omega\epsilon}[j_{x,\mathbf{G}}^{\rm 1D}+j_{x,\mathbf{G}}^{\rm 2D}\exp(-\kappa_G D)], \tag{8}$$

$$B_{\mathbf{G}}=\frac{2\pi i\kappa_G}{\omega\epsilon}[j_{x,\mathbf{G}}^{\rm 1D}-j_{x,\mathbf{G}}^{\rm 2D}\exp(-\kappa_G D)], \tag{9}$$

$$D_{\mathbf{G}}=-\frac{2\pi i\kappa_G}{\omega\epsilon}[j_{x,\mathbf{G}}^{\rm 1D}+j_{x,\mathbf{G}}^{\rm 2D}\exp(\kappa_G D)]. \tag{10}$$

Together with the relation

$$j_{x,\mathbf{G}}^{\rm 2D}=\sigma_{\rm 2D}(\mathbf{G},\omega)E_{x,\mathbf{G}}^{\rm tot}|_{z=D}, \tag{11}$$

between the current in the 2DES and the total electric field at the plane $z=D$ we have five equations for six unknowns $A_{\mathbf{G}},\ldots,D_{\mathbf{G}},j_{x,\mathbf{G}}^{\rm 1D},j_{x,\mathbf{G}}^{\rm 2D}$. Using these equations we relate the total field at the plane $z=0$ to the current $j_{x,\mathbf{G}}^{\rm 1D}$ at the same plane,

$$E_{x,\mathbf{G}}^{\rm tot}|_{z=0}=W(\mathbf{G},\omega)\left(E_{x,\mathbf{G}}^{\rm ext}|_{z=0}-\frac{2\pi i\kappa_G}{\omega\epsilon}j_{x,\mathbf{G}}^{\rm 1D}\right), \tag{12}$$

where

$$W(\mathbf{G},\omega)=1-\left(1-\frac{1}{\epsilon_{\rm 2D}(\mathbf{G},\omega)}\right)e^{-2\kappa_G D}, \tag{13}$$

and

$$\epsilon_{\rm 2D}(\mathbf{G},\omega)=1+\frac{2\pi i\kappa_G}{\omega\epsilon}\sigma_{\rm 2D}(\mathbf{G},\omega) \tag{14}$$

is the (relative) ''dielectric permittivity'' of the 2DES.

Properties of the grating should now be introduced into the theory. Usually[16–18] one assumes the local Ohm's law for the grating, $j_x^{\rm 1D}(x)=\sigma_{\rm 1D}(x,\omega)E_x^{\rm tot}(x,z=0)$, where the conductivity $\sigma_{\rm 1D}(x,\omega)$ is proportional to the local electron density (1). Then Eq. (12) is rewritten in the form of an integral equation,

$$E_x^{\rm tot}(x)=E_0 W(\mathbf{0},\omega)+\left(\frac{\partial^2}{\partial x^2}+\frac{\omega^2\epsilon}{c^2}\right)\times\int\frac{dx'}{W}\vartheta(x')L(x-x')E_x^{\rm tot}(x'), \tag{15}$$

where

$$E_x^{\rm tot}(x)\equiv E_x^{\rm tot}(x,z=0),\quad \vartheta(x)=n_1(x)/\langle n_1(x)\rangle$$

is a normalized electron density in a grating strip, the kernel $L(x-x')$ is defined as

$$L(x-x')=\frac{2\pi i f\langle\sigma_{\rm 1D}(\omega)\rangle}{\omega\epsilon}\sum_{\mathbf{G}}\frac{W(\mathbf{G},\omega)}{\kappa_G}e^{i\mathbf{G}\cdot(\mathbf{r}-\mathbf{r}')}, \tag{16}$$

$f=W/a$ is the geometrical ''filling factor'' of the grating, and the angular brackets mean the average over the area of a grating strip, $\langle\cdots\rangle=\int(\cdots)dx/W$.

A general scheme of solving Eq. (15) is presented in Appendix A. Here we solve this equation approximately,[19–21] assuming that the total (and induced) electric field *inside* the strips is uniform, $E_x^{\rm inside}\equiv E_x^{\rm tot}(|x|<W/2,z=0)=\text{const}$. This approximation works very well in a metal grating if the frequency of electromagnetic wave is small as compared to the plasma frequency of the metal, and the width of the grating strips is large as compared to the Thomas-Fermi screening length. Under these conditions the electric field inside the strips is completely screened and $E_x^{\rm inside}=\text{const}=0$. This approximation is also valid in a quantum wire (quantum dot) grating at an arbitrary frequency, if the wires (dots) are considered in an oblate cylinder[23] (oblate spheroid[24]) model. This follows from the well-known fact that an internal electric field in an arbitrary ellipsoid is uniform if the external one is uniform.[25] This is also valid for wires or dots formed by a parabolic confining potential.[26] The validity of the model has been recently checked using a number of numerical approaches in Ref. 27. It has been shown that the model gives reliable results for experimentally measured (macroscopic) values like for instance the transmission coefficient.

Assuming that $E_x^{\rm inside}=\text{const}$, we get a relation between the total electric field inside the grating strips and the external field (see Appendix A). It has a form of a response equation

$$E_x^{\rm inside}=\frac{E_0}{\zeta(\omega)}, \tag{17}$$

where the response function $\zeta(\omega)$ is given by

$$\zeta(\omega)=\frac{1}{W(\mathbf{0},\omega)}\left(1+\frac{2\pi i f\langle\sigma_{1D}(\omega)\rangle}{\omega\epsilon}\times\sum_{\mathbf{G}}\kappa_G\alpha(\mathbf{G})W(\mathbf{G},\omega)\right). \quad (18)$$

The form factor in Eq. (18),

$$\alpha(\mathbf{G})=|\langle\vartheta(x)e^{i\mathbf{G}\cdot\mathbf{r}}\rangle|^2, \quad (19)$$

is determined by Fourier components of the equilibrium electron density in the grating strips.

The response equation (17) and the response function (18) are the main points of our theory. Having derived these equations we can now calculate fields and currents in all the space. In particular, for Fourier amplitudes of electric fields at $z<0$ and $z>D$, which describe the reflected and transmitted field in all diffraction orders as well as the evanescent field, we get

$$\frac{A_{\mathbf{G}}}{E_0}=-\delta_{\mathbf{G},\mathbf{0}}+W(\mathbf{G},\omega)\times\left(\delta_{\mathbf{G},\mathbf{0}}-\frac{2\pi i f\kappa_G\langle\sigma_{1D}(\omega)\rangle\langle\vartheta(x)e^{-i\mathbf{G}\cdot\mathbf{r}}\rangle}{\omega\epsilon\zeta(\omega)}\right), \quad (20)$$

$$\frac{D_{\mathbf{G}}}{E_0}=-\delta_{\mathbf{G},\mathbf{0}}+\frac{1}{\epsilon_{2D}(\mathbf{G},\omega)}\times\left(\delta_{\mathbf{G},\mathbf{0}}-\frac{2\pi i f\kappa_G\langle\sigma_{1D}(\omega)\rangle\langle\vartheta(x)e^{-i\mathbf{G}\cdot\mathbf{r}}\rangle}{\omega\epsilon\zeta(\omega)}\right). \quad (21)$$

Equations (20),(21) give the general solution of the formulated problem. They have been derived under quite general assumptions and include both the electrodynamics of the grating coupler and nonlocal and quantum-mechanical effects in the response of the 2DES's that enter the theory via an appropriate model of the conductivity $\sigma_{2D}(\mathbf{G},\omega)$. In subsequent sections we apply the general theory to the problem of FIR response of the system ''grating coupler–2DES with and without a flowing current.''

III. THEORY OF THE GRATING COUPLER: TRANSMISSION OF FIR RADIATION

A. Approximations and preliminary notes

Before applying the general results of Sec. II to the problem of FIR response of the grating coupled 2DES we specify the conditions of a typical experiment and make necessary approximations. First, we assume that the grating period a is small as compared to the wavelength of light λ (in a typical experimental situation $\lambda\sim 300\ \mu$m, $a\lesssim 1\ \mu$m). Under this condition only the $\mathbf{G}=\mathbf{0}$ components of the electric field describe outgoing waves, while all components with $\mathbf{G}\neq\mathbf{0}$ are evanescent. The reflection $r(\omega)$ and transmission $t(\omega)$ amplitudes are then determined by the coefficients $A_{\mathbf{G}=\mathbf{0}}$ and $D_{\mathbf{G}=\mathbf{0}}$, respectively, and we have

$$r(\omega)=-1+W(\mathbf{0},\omega)\left(1-\frac{2\pi f\langle\sigma_{1D}(\omega)\rangle}{c\sqrt{\epsilon}\zeta(\omega)}\right), \quad (22)$$

$$t(\omega)=\frac{1}{\epsilon_{2D}(\mathbf{0},\omega)}\left(1-\frac{2\pi f\langle\sigma_{1D}(\omega)\rangle}{c\sqrt{\epsilon}\zeta(\omega)}\right), \quad (23)$$

where $\epsilon_{2D}(\mathbf{0},\omega)=1+2\pi\sigma_{2D}(\mathbf{0},\omega)/c\sqrt{\epsilon}$. The reflection, transmission, and absorption coefficients are then determined, as usual, by the relations[28]

$$R(\omega)=|r(\omega)|^2,\quad T(\omega)=|t(\omega)|^2, \quad (24)$$

$$A(\omega)=1-R(\omega)-T(\omega). \quad (25)$$

Second, we assume that the distance D between the 2DES and the grating is also small as compared to λ. Then $W(\mathbf{0},\omega)=\epsilon_{2D}^{-1}(\mathbf{0},\omega)$, and

$$r(\omega)=-1+t(\omega), \quad (26)$$

where $t(\omega)$ is given by Eq. (23).

Third, we specify the model for the conductivity of the 2DES. We postpone an analysis of the nonlocal and quantum-mechanical effects in the 2DES to a subsequent publication, and describe the properties of the 2DES in the hydrodynamic model[29] of $\sigma_{2D}(\mathbf{q},\omega)$. Linearizing the continuity and Euler's equations[30] for the density n and the velocity $\mathbf{v}$ of 2D electrons,

$$\frac{\partial n}{\partial t}+\nabla(n\mathbf{v})=0, \quad (27)$$

$$\frac{\partial\mathbf{v}}{\partial t}+(\mathbf{v}\cdot\nabla)\mathbf{v}=-\frac{e}{m_2}\mathbf{E}-\gamma_2(\mathbf{v}-\mathbf{v}_{dr}), \quad (28)$$

where $\mathbf{E}=\mathbf{E}_0+\delta\mathbf{E}$, $n=n_2+\delta n$, $\mathbf{v}=\mathbf{v}_{dr}+\delta\mathbf{v}$, we get $\mathbf{v}_{dr}=-(e/m_2\gamma_2)\mathbf{E}_0$, and

$$\sigma_{2D}(\mathbf{q},\omega)=\frac{n_2e^2}{m_2}\frac{i\omega}{(\omega-\mathbf{q}\mathbf{v}_{dr})(\omega-\mathbf{q}\mathbf{v}_{dr}+i\gamma_2)}. \quad (29)$$

For the average conductivity of the grating we assume, similarly,

$$\langle\sigma_{1D}(\omega)\rangle=\frac{n_1e^2}{m_1}\frac{i}{\omega+i\gamma_1}. \quad (30)$$

In Eqs. (28)–(30) n_i, m_i, and γ_i are the average electron density, the electron effective mass, and the momentum relaxation rate in the grating ($i=1$) and in the 2DES ($i=2$), respectively.

Substituting the model expressions (29),(30) for the conductivity of the 2DES and the grating into Eq. (23) we get the following result for the transmission amplitude:[21]

$$t(\omega)=\frac{\omega+i\gamma_2}{\omega+i\gamma_2+i\Gamma_2}\left(1-\frac{i\Gamma_1}{\omega+i\gamma_1}\frac{1}{\zeta(\omega)}\right), \quad (31)$$

where the response function assumes the form

$$\zeta(\omega)=\frac{i\Gamma_1}{\omega+i\gamma_1}+\left(1+\frac{i\Gamma_2}{\omega+i\gamma_2}\right)\times\left\{1-\frac{\tilde{\omega}_{p1}^2}{\omega(\omega+i\gamma_1)}\left[1+\frac{2\pi f n_1 e^2}{m_1\epsilon\tilde{\omega}_{p1}^2}\times\sum_{m\neq 0}\frac{|G_m|\alpha(G_m)e^{-2|G_m|D}\omega_{p2}^2(G_m)}{(\omega-G_m v_{\rm dr})(\omega-G_m v_{\rm dr}+i\gamma_2)-\omega_{p2}^2(G_m)}\right]\right\}. \tag{32}$$

Here

$$\omega_{p2}(G_m)=\left(\frac{2\pi n_2 e^2|G_m|}{m_2\epsilon}\right)^{1/2} \tag{33}$$

is the frequency of 2D plasmons, $G_m=2\pi m/a$,

$$\Gamma_1=\frac{2\pi f n_1 e^2}{m_1 c\sqrt{\epsilon}}, \tag{34}$$

$$\Gamma_2=\frac{2\pi n_2 e^2}{m_2 c\sqrt{\epsilon}}, \tag{35}$$

and

$$\tilde{\omega}_{p1}^2=\frac{2\pi f n_1 e^2}{m_1\epsilon}\sum_{m\neq 0}|G_m|\alpha(G_m). \tag{36}$$

The physical meaning of the values Γ_1, Γ_2, and $\tilde{\omega}_{p1}$ will be discussed in Sec. III B.

Finally, we specify the density profile function $\vartheta(x)$ that determines the form factor $\alpha(\mathbf{G})$. In the main part of the paper we will use a semielliptic density profile,

$$\vartheta(x)=\frac{4}{\pi}[1-(2x/W)^2]^{1/2}, \tag{37}$$

for which the form factor $\alpha(G_m)$ is given by

$$\alpha(G_m)=[2J_1(z)/z]^2,\quad z=G_m W/2, \tag{38}$$

where J_1 in the Bessel function. In some cases we will also consider a steplike profile, $\vartheta_{\rm step}(x)=\theta(W/2-|x|)$, for which

$$\alpha_{\rm step}(G_m)=(\sin z/z)^2,\quad z=G_m W/2. \tag{39}$$

Using Eqs. (31), (32), as well as Eqs. (24) and (25), one can show that the functions $T(\omega)$, $R(\omega)$, and $A(\omega)$ have one or more resonant features related with an excitation of plasma modes in the system. The resonance frequencies and linewidths depend on the drift velocity of 2D electrons $v_{\rm dr}$, as well as on other physical and geometrical parameters of the structure. If a resonant feature is well separated from others, i.e., when its linewidth is small as compared to the distance between adjacent resonances, the functions $T(\omega)$, $R(\omega)$, and $A(\omega)$ assume the following general form:

$$T(\omega)=1-\frac{\omega^2(2\gamma\Gamma+\Gamma^2)}{(\omega^2-\Omega^2)^2+\omega^2(\gamma+\Gamma)^2}, \tag{40a}$$

$$R(\omega)=\frac{\omega^2\Gamma^2}{(\omega^2-\Omega^2)^2+\omega^2(\gamma+\Gamma)^2}, \tag{40b}$$

$$A(\omega)=\frac{2\omega^2\gamma\Gamma}{(\omega^2-\Omega^2)^2+\omega^2(\gamma+\Gamma)^2}, \tag{40c}$$

where Ω is the resonance frequency; γ and Γ are the nonradiative and the radiative decay rates, respectively. The total linewidth of the resonance is thus determined by the sum of the radiative and the nonradiative decay rates; the resonant values of the transmission, reflection, and absorption coefficients, $T_{\rm res}\equiv T(\Omega)$, $R_{\rm res}\equiv R(\Omega)$, $A_{\rm res}\equiv A(\Omega)$, are determined by the ratio γ/Γ,

$$T_{\rm res}=\frac{\gamma^2}{(\gamma+\Gamma)^2},\quad R_{\rm res}=\frac{\Gamma^2}{(\gamma+\Gamma)^2},\quad A_{\rm res}=\frac{2\gamma\Gamma}{(\gamma+\Gamma)^2}. \tag{41}$$

The resonant values (41) characterize the strength of the resonant features. Note that the reflection (absorption) resonant amplitude is negligible as compared to the absorption (reflection) amplitude if $\Gamma\ll\gamma$ ($\Gamma\gg\gamma$). In the following, we specify the values of Ω, γ, and Γ in different considered cases.

The rest of this section is devoted to an analysis of the system without flowing current, i.e., at $v_{\rm dr}=0$. In Sec. IV we analyze the general formulas at a finite drift velocity.

B. Two limiting cases

We start our analysis from two simple limiting cases, of a 2DES without grating coupler and of a grating without the 2DES.

1. 2DES without grating

If the grating is absent, then $\Gamma_1=0$, and the transmission, reflection, and absorption coefficients assume the form (40) with

$$\Omega=0,\quad \gamma=\gamma_2,\quad \Gamma=\Gamma_2. \tag{42}$$

The nonradiative contribution to the linewidth γ is determined by the momentum relaxation rate of 2D electrons γ_2 and is due to the Drude absorption in the 2DES. The physical meaning of the value Γ_2, Eq. (35), is the radiative decay of oscillating 2D electrons in the 2DES taken in isolation (without the grating). Indeed, if one electron is placed in an electric field $E_0\exp(-i\omega t)$, it oscillates with an amplitude $\delta x\sim eE_0/m\omega^2$. This creates an oscillating dipole moment $d\sim e^2E_0/m\omega^2$, which produces a dipole radiation[31] with the intensity $I\sim\omega^4d^2/c^3$. Dividing the radiated intensity I by the average energy of the oscillating dipole $W\sim m\omega^2\delta x^2$ one gets the radiative decay of a *single* electron $\Gamma_0\sim e^2\omega^2/mc^3$. When a *sheet of electrons* with an area density n_s is placed in an oscillating electric field, and the interelectron distance n_s^{-1} is small as compared to the wavelength of light λ, all $N\sim n_s\lambda^2$ electrons within the coherence area $\sim\lambda\times\lambda$ radiate in phase. The average energy should then be multiplied by a factor of N, while the radiated intensity by a factor of N^2. The radiative decay of an electron sheet is then given by the product $\Gamma_0 N\sim\Gamma_0 n_s\lambda^2\sim n_s e^2/mc$ in agreement with the exact expression (35).

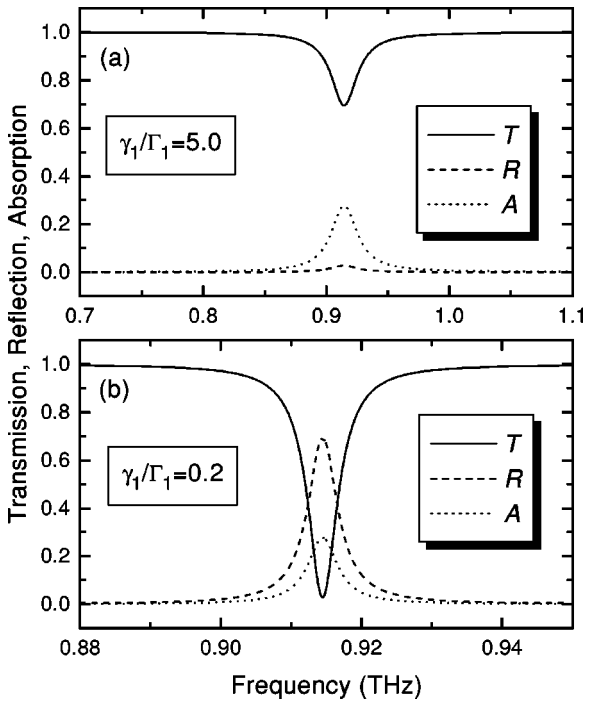

FIG. 2. The transmission, reflection, and absorption coefficients of a quantum-wire grating with $n_1=3\times10^{11}$ cm^{-2}, $m_1=0.067$ (GaAs), and two different values of the relaxation rate: (a) $\gamma_1=1.33\times10^{11}$ s^{-1} (corresponds to $\gamma_1/\Gamma_1=5.0$), and (b) $\gamma_1=0.53\times10^{10}$ s^{-1} ($\gamma_1/\Gamma_1=0.2$). The ratio $W/a=0.4$.

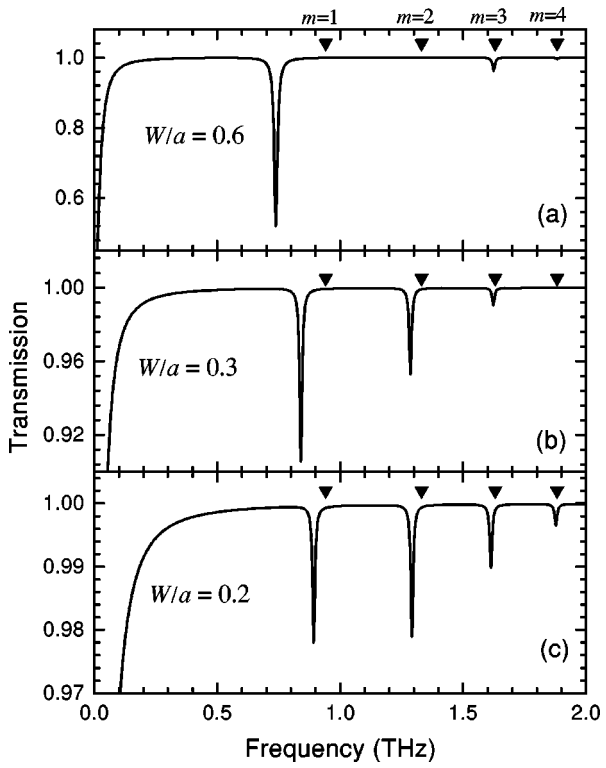

FIG. 3. The transmission coefficient of the structure metal grating–2DES at three different values of the ratio W/a. Geometrical parameters: $a=1$ μm, $D=60$ nm. Parameters of the 2D layer: $n_{s2}=3\times10^{11}$ cm^{-2}, $\gamma_2=0.7\times10^{11}$ s^{-1}, $m_2=0.067$ (mobility $\mu_2=375\,000$ cm^2/V s). The grating parameters ($n_{s1}=6\times10^{18}$ cm^{-2}, $\gamma_1=1.1\times10^{14}$ s^{-1}, $m_1=1$) correspond to a typical (Au) grating coupler. The dielectric constant is $\epsilon=12.8$. Triangles show the calculated positions of the 2D plasmon harmonics (33) for $m=1,\ldots,4$. Note the differences in the vertical axis scales for different plots.

2. Grating without 2DES

If the 2DES is absent, then $\Gamma_2=\omega_{p2}(G_m)=0$, and the transmission, reflection, and absorption coefficients assume the form (40) with

$$\Omega=\tilde{\omega}_{p1},\quad \gamma=\gamma_1,\quad \Gamma=\Gamma_1. \tag{43}$$

The nonradiative contribution to the linewidth γ_1 is now due to the Drude absorption in the grating strips. The value Γ_1 is proportional to the average electron density in the grating fn_1, Eq. (34), and is the radiative decay of plasma oscillations in the grating taken in isolation (with the removed 2DES). The value $\tilde{\omega}_{p1}$ gives the resonance frequency of plasmons in a periodic array of grating strips (or quantum wires). Eq. (36) provides a functional dependence of $\tilde{\omega}_{p1}$ on the equilibrium electron density $\vartheta(x)$ in wires (similar functional dependencies for arrays of quantum dots and antidots have been found in Refs. 19 and 32, respectively). If the equilibrium electron density in strips has a semielliptic form (37), Eq. (36) gives (see Appendix B)

$$\tilde{\omega}_{p1}^2=\omega_{p1}^2\beta(f)\equiv\omega_{p1}^2\left[1-\frac{(\pi f)^2}{24}-\frac{(\pi f)^4}{960}\right], \tag{44}$$

where

$$\omega_{p1}=\sqrt{\frac{16n_1e^2}{m_1\epsilon W}} \tag{45}$$

is the resonance frequency of plasmons in a single wire, and the factor $\beta(f)$ is due to the interwire interaction. If the wire is formed by an external *parabolic* confining potential $V_{\rm ext}(x)=Kx^2/2$, Eq. (36) reproduces an exact result $\omega_{p1}^2=K/m_1$ of the generalized Kohn theorem,[33] see Appendix B.

Figure 2 shows the frequency dependencies of the transmission, reflection, and absorption coefficients of a quantum wire array at two ratios of the collisional damping to the radiative decay, $\gamma_1/\Gamma_1\gg1$ [Fig. 2(a)] and $\gamma_1/\Gamma_1\ll1$ [Fig. 2(b)]. In the former case the reflection of waves is negligibly small, and the transmission minimum is due to a peak in the absorption coefficient. In the latter case, the absorption of waves is small as compared to their reflection, and the transmission minimum is mainly due to the reflection peak. The width of the resonance in the second case is smaller than that in the first case (but does not tend to zero) and is determined mainly by the radiative decay.

C. Grating coupled 2DES

Now we consider the transmission of FIR radiation through a coupled structure ''grating–2DES'', under the condition when no current is flowing in the 2DES ($v_{\rm dr}=0$). We consider two different cases: the case of a *metal* grating, when the plasma frequency in the grating $\tilde{\omega}_{p1}$ is much larger (several orders of magnitude in a typical experiment) than the 2D plasmon frequency $\omega_{p2}(G_1)$, and the case

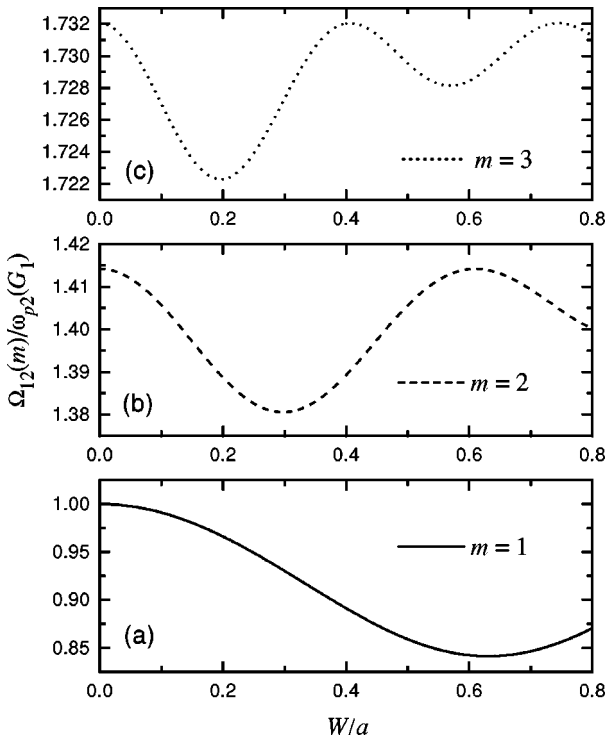

FIG. 4. Normalized resonance frequencies $\Omega_{12}(m)/\omega_{p2}(G_1)$ for three different modes $m=1$, 2, and 3 as a function of the geometrical filling factor $f=W/a$. The ratio $D/a=0.08$. Note the differences in the vertical axis scales for different modes.

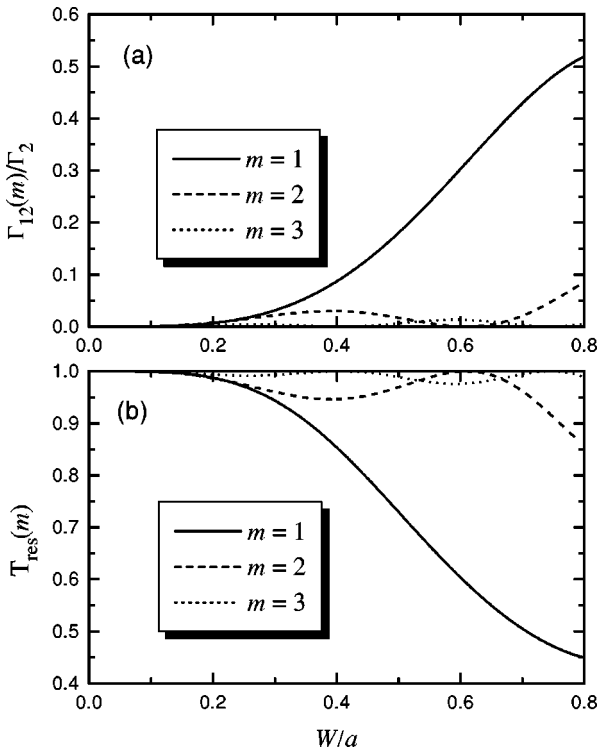

FIG. 5. (a) Normalized radiative decay of the modes $\Omega_{12}(m)$ and (b) the resonant transmission coefficient $T_{\rm res}(m)$, for three different modes $m=1$, 2, and 3 as a function of the geometrical filling factor $f=W/a$. The ratio $D/a=0.08$; the scattering rate of electrons in the 2DES [in (b)] is $\gamma_2=0.7\times10^{11}$ s^{-1}.

of a *quantum-wire* grating, when the plasma frequencies in the grating and in the 2DES are of the same order of magnitude.

1. Metal grating

Figure 3 demonstrates the frequency dependent transmission coefficient of the structure ''metal grating–2DES'' at different values of the geometrical filling factor of the grating f. Three characteristic features are seen in the figure. First, the position of resonances that we denote as $\Omega_{12}(m)$ does not coincide with the frequencies of the 2D plasmons $\omega_{p2}(G_m)$, Eq. (33), shown in Fig. 3 by triangles for four lowest harmonics $m=1,2,3,4$. The index ''12'' here is a reminder that we are dealing with the *coupled* 1D (grating)–2D electron system. Second, the position and the amplitude of resonances for different m essentially depend on the filling factor $f=W/a$. At some values of f the amplitude of higher harmonics can be comparable with or even larger than those of lower harmonics (as is the case for the modes $m=1$ and $m=2$ at $W/a=0.2$, Fig. 3(c), or for the modes $m=2$ and $m=3$ at $W/a=0.6$, Fig. 3(a). At certain values of f some harmonics are not excited at all (e.g., the mode $m=2$ at $W/a=0.6$, Fig. 3(a). Third, the amplitudes of the transmission resonances become smaller when the resonance positions $\Omega_{12}(m)$ approach the 2D plasmon frequencies $\omega_{p2}(G_m)$, see, e.g., the evolution of the $\Omega_{12}(1)$ mode amplitude with decreasing W/a [note the difference in the vertical axis scales in Figures 3(a)–3(c)].

In order to understand these features we take the limits $v_{\rm dr}=0$ (no drift) and $n_1\to\infty$ (metal grating) in the general formulas (31) and (32). The resulting expressions for the transmission, reflection, and absorption coefficients near the resonance $\omega=\Omega_{12}(m)$ assume the form (40) where

$$\Omega^2=\Omega_{12}^2(m)\equiv\omega_{p2}^2(G_m)(1-\Delta_m), \tag{46}$$

$$\Gamma=\Gamma_{12}(m)\equiv\frac{\Gamma_1}{\tilde{\omega}_{p1}^2}\omega_{p2}^2(G_m)\Delta_m=\Gamma_2\frac{(\pi f)^2}{4\beta(f)}|m|\Delta_m, \tag{47}$$

and $\gamma=\gamma_2$. The parameter

$$\Delta_m=\frac{(\pi f)^2}{2\beta(f)}|m|\alpha(G_m)\exp(-2|G_m|D) \tag{48}$$

here depends on the harmonic index m and on geometrical parameters of the structure. Note that the physical parameters of the grating—the electron density n_1, the momentum relaxation rate γ_1, and the effective mass m_1—do not enter the formulas (46)–(48), in which the grating is presented only via the geometrical parameters a, W, and D. The resonant values of the transmission, reflection, and absorption coefficients, $T_{\rm res}(m)$, $R_{\rm res}(m)$, and $A_{\rm res}(m)$, are determined by Eq. (41) where $\gamma=\gamma_2$ and $\Gamma=\Gamma_{12}(m)$.

As seen from Eqs. (46), (47), and (41), the resonance frequency, the radiative contribution to the linewidth, and the strength of the resonance essentially depend on the parameter Δ_m, which exponentially decreases with the distance D between the 2DES and the grating and oscillates as a function of the grating filling factor f [via the oscillating f dependence of the form factor $\alpha(G_m)$, Eqs. (38),(39)]. If Δ_m tends to zero, the resonance frequencies $\Omega_{12}(m)$ tend to the 2D

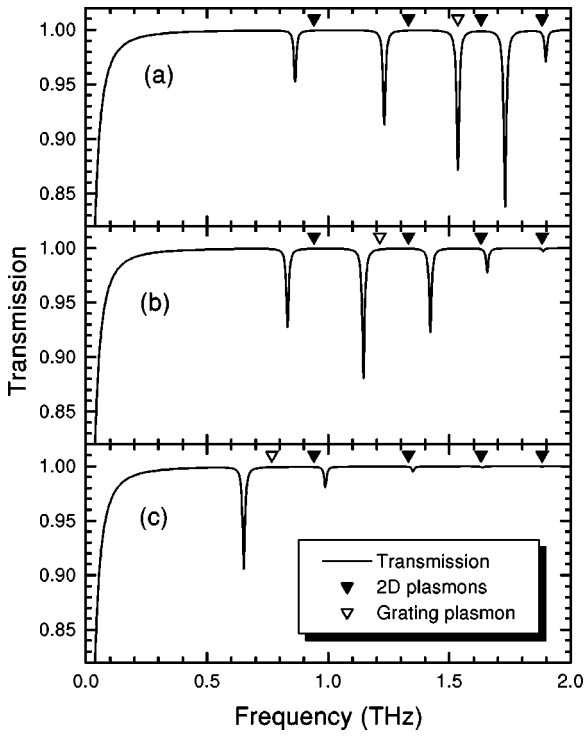

FIG. 6. The transmission coefficient of the structure quantum-wire grating–2DES at three different values of the grating plasmon frequency $\tilde{\omega}_{p1}$ at $a=1$ μm, $D=60$ nm, and $W=0.2$ μm. Parameters of the 2D layer and the dielectric constant ϵ are the same as in Fig. 3. The parameters of the grating are $\gamma_1=0.7\times10^{11}$ s^{-1}, $m_1^*=0.067$; and the electron density: (a) $n_{s1}=4\times10^{11}$ cm^{-2}, (b) $n_{s1}=2.5\times10^{11}$ cm^{-2}, and (c) $n_{s1}=1\times10^{11}$ cm^{-2}. Triangles show the calculated positions of the 2D plasmon harmonics (33) for $m=1,\ldots,4$, open triangles show the positions of the grating plasmon (44).

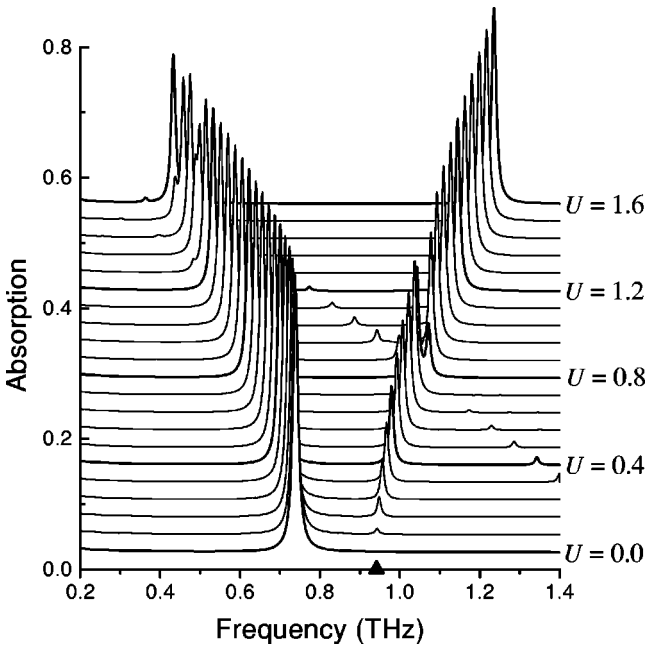

FIG. 7. The absorption coefficient of the structure metal grating–2DES at the frequency interval corresponding to the first ($m=1$) 2D plasmon harmonic, and at small values of the dimensionless drift velocity $U=v_{\rm dr}/v_{F2}$. Physical and geometrical parameters of the structure are the same as in Fig. 3(a). The black triangle at the bottom of the plot shows the position of the $m=1$, 2D plasmon harmonic (33). The weak mode that intersects the pronounced resonances at $U\approx0.8$ and $U\approx1.5$ is the mode $(3,-)$.

plasmon frequencies $\omega_{p2}(G_m)$, but the radiative decay and the strength of the resonances vanish, $\Gamma_{12}(m)=0$, $T_{\rm res}(m)=1$. The value of Δ_m vanishes when πfm coincides with any of zeros of the Bessel function J_1, for a semielliptic density profile (37), or with any of zeros of the sine function, for a steplike profile. In order to get the maximum strength of the mth plasma resonance one should thus satisfy the condition $J_1^2(\pi fm)=$maximum (a semielliptic profile), or

$$\frac{W}{a}m=0.57, \quad \frac{W}{a}m=1.7, \tag{49}$$

etc. Figures 4 and 5 demonstrate the f dependencies of the resonance frequencies $\Omega_{12}(m)$ [normalized by $\omega_{p2}(G_1)$], radiative contribution to the linewidth $\Gamma_{12}(m)$ (normalized by Γ_2), and the resonant transmission coefficient $T_{\rm res}(m)$ for three lowest modes $m=1$, 2, and 3 at $D/a=0.08$, for the semielliptic density profile (37). The behavior of $\Omega_{12}(m)$, $\Gamma_{12}(m)$, and $T_{\rm res}(m)$ at the steplike profile is qualitatively the same.

2. Quantum-wire grating

If the grating coupler is made out of a metal, only the geometrical (but not the physical) parameters of the grating determine the observable transmission (reflection, absorption) resonances. If the grating is made out of a 2D electron layer with *similar* plasma parameters (the quantum-wire grating) the observable resonances are determined by both the 2D plasmons in the 2DES, and the plasma modes in the grating. This gives additional possibilities to control the transmission spectra, especially in the finite drift velocity regime (Sec. IV).

Figure 6 shows the transmission coefficient $T(\omega)$ of the structure ''*quantum-wire* grating–2DES'' at three different values of the grating plasma frequency $\tilde{\omega}_{p1}$. Geometrical parameters of the structure are the same as in Fig. 3(c), where the transmission coefficient of the *metal* grating-coupled 2DES is shown. Three new features are seen in Fig. 6 as compared to Fig. 3(c). First, due to the presence of the grating plasmon resonance $\tilde{\omega}_{p1}$ an additional resonance peak appears in the plot. Second, due to the interaction of 2D plasmons and the grating plasmon the resonance peaks are slightly shifted relative to their positions in Fig. 3(c). Third, and the most important feature, is a dramatic enhancement of the amplitudes of the 2D plasmon resonances, in situations when the frequency $\tilde{\omega}_{p1}$ approaches the 2D plasmon frequencies, Figs. 6(a),6(b). This effect is due to a resonant interaction of the grating plasmon with the 2D ones, and is especially pronounced for higher 2D plasmon modes, for which the amplitude of resonances is increased by about an order of magnitude [note the difference in the vertical axis scales in Figs. 6 and 3(c)]. This effect is of a particular importance in the 2DES with a flowing current, as it allows one to increase the amplification and to reduce the threshold velocity in the structure with the quantum wire grating (Sec. IV B).

IV. AMPLIFICATION OF WAVES

Now we analyze the transmission of electromagnetic waves through a grating-coupled 2DES with a flowing current. We start from the case of a structure ''metal grating–2DES.''

A. Metal grating

Figure 7 shows the absorption coefficient of the structure ''metal grating–2DES'' at relatively small values of the dc current ($U \equiv v_{dr}/v_{F2} \leqslant 1.6$) in the frequency interval corresponding to an excitation of the first ($m=1$) 2D plasmon harmonic. Here v_{F2} is the Fermi velocity of 2D electrons in the 2DES. The physical and geometrical parameters of the structure are the same as in Fig. 3(a) ($W/a=0.6$). The triangle at the bottom of the plot shows the position of the $m=1$ 2D plasmon harmonic (33). As seen from Fig. 7, in contrast to the case of the vanishing current ($U=0$, lower curve), at finite drift velocities of 2D electrons there are two modes, $\Omega_{12}(m,\pm)$, associated with each harmonic number m. We label these modes by two indexes $(m,\pm)$, where the frequency of the $+(-)$ mode increases (decreases) with v_{dr} at small v_{dr}, $d\Omega_{12}(m,+)/dv_{dr}>0$ and $d\Omega_{12}(m,-)/dv_{dr}<0$ at $v_{dr}\to 0$. As seen from the figure,

$$\lim_{v_{dr}\to 0} \Omega_{12}(m,+) = \omega_{p2}(G_m), \tag{50}$$

$$\lim_{v_{dr}\to 0} \Omega_{12}(m,-) = \Omega_{12}(m), \tag{51}$$

where $\Omega_{12}(m)$ is defined in Eq. (46). The strength of the $(m,+)$ mode vanishes when the drift velocity tends to zero.

In order to get a quantitative description of the resonant features shown on Fig. 7 we take the limit $n_1 \to \infty$ (metal grating) in the general formulas (31)–(32). Assuming that $|\omega + i\gamma_2| \gg \Gamma_2$ and $\omega_{p2}(G_m) \gg \gamma_2$, and taking into account only the terms with $m = \pm|m|$ in the sum in Eq. (32), we find that near the $(m,\pm)$ resonance the transmission, reflection, and absorption coefficients assume the form (40), where the resonance frequency $\Omega = \Omega_{12}(m,\pm)$ is determined by the equation

$$\Omega_{12}^2(m,\pm) = \omega_{p2}^2(G_m)\left(1-\frac{\Delta_m}{2}\right) + (G_m v_{dr})^2 \pm \omega_{p2}(G_m) \times \sqrt{\omega_{p2}^2(G_m)\left(\frac{\Delta_m}{2}\right)^2 + (2G_m v_{dr})^2\left(1-\frac{\Delta_m}{2}\right)}, \tag{52}$$

the radiative decay $\Gamma = \Gamma_{12}(m,\pm)$ is given by

$$\Gamma_{12}(m,\pm) = \frac{\Gamma_{12}(m)}{2}\left\{1 \mp \frac{\omega_{p2}^2(G_m)\Delta_m - (2G_m v_{dr})^2}{\omega_{p2}(G_m)\sqrt{\omega_{p2}^2(G_m)\Delta_m^2 + (4G_m v_{dr})^2(1-\Delta_m/2)}}\right\}, \tag{53}$$

and the nonradiative decay $\gamma = \gamma_2$. Figure 8 shows the drift velocity dependencies of the resonance frequency $\Omega_{12}(m,\pm)$ and the normalized radiative decay $\Gamma_{12}(m,\pm)/\Gamma_{12}(m)$ for the mode $m=1$ at parameters of Fig. 3(a). The frequency $\Omega_{12}(m,+)[\Omega_{12}(m,-)]$ increases (decreases) with the square of the drift velocity at $G_m v_{dr} \ll \omega_{p2}(G_m)\Delta_m/4$, and linearly,

$$\Omega_{12}(m,\pm) \approx |\omega_{p2}(G_m)\sqrt{1-\Delta_m/2} \pm G_m v_{dr}|, \tag{54}$$

at $G_m v_{dr} \gg \omega_{p2}(G_m)\Delta_m/4$ (the Doppler shifted plasma resonances). In the region $\omega_{p2}(G_m)\sqrt{1-\Delta_m} < G_m v_{dr} < \omega_{p2}(G_m)$ the frequency $\Omega_{12}(m,-)$ vanishes, and at $G_m v_{dr} > \omega_{p2}(G_m)$ it increases again with the positive slope, $d\Omega_{12}(m,-)/dv_{dr}>0$ at $G_m v_{dr} > \omega_{p2}(G_m)$.[34] The radiative decay, as well as the strength of the $\Omega_{12}(m,+)$ resonance, equal zero at $v_{dr}=0$ and increase monotonously when the drift velocity increases [Fig. 8(b)]. The radiative decay of the $\Omega_{12}(m,-)$ mode decreases from a finite value at $v_{dr}=0$, vanishes at $G_m v_{dr} = \omega_{p2}(G_m)$, and *changes its sign* at $G_m v_{dr} > \omega_{p2}(G_m)$. As seen from Eqs. (41), when Γ equals zero, the reflection and absorption coefficients at the resonance $\omega = \Omega$ disappear, and the transmission coefficient equals unity. When Γ becomes negative, the resonant transmission coefficient exceeds unity, which means an amplification of waves, while the absorption coefficient becomes negative, which means that the energy is transfered not from the electromagnetic wave to the electron system, but conversely, from the current driven electron system (eventually from the battery that supplies the current) to the electromagnetic wave. The plasma mode $\Omega_{12}(m,-)$ thus becomes unstable at $G_m v_{dr} > \omega_{p2}(G_m)$.[15] Figure 9 demonstrates the drift velocity dependencies of the transmission, reflection, and absorption coefficients at the resonance $\omega = \Omega_{12}(m,\pm)$ for $m=1$. An amplification of the transmitted electromagnetic waves is explicitly demonstrated in Fig. 10 where we draw the frequency dependence of the transmission coefficient at different drift velocities at a larger range (as compared with Fig. 7) of $v_{dr}(0 \leqslant U \leqslant 8)$.

In the above calculations we have assumed that the resonance at $\omega = \Omega_{12}(m,\pm)$ is well separated from other resonances (i.e., that the width of the resonance line is small as compared to the distance to neighbor resonances). There are two effects in which this approximation is insufficient. The first one concerns an accurate evaluation of the threshold velocity of the amplification of waves. We define the threshold velocity v_{th} by the condition $T_{res}>1$. As follows from the above discussion and Fig. 9, the resonant transmission coefficient exceeds unity when $G_m v_{dr} > \omega_{p2}(G_m)$. This inequality gives, however, only the lower estimate for the v_{th}. In order to evaluate the threshold velocity more accurately one should take into account that the amplification of waves should exceed the Drude absorption in the 2DES (Sec. III B 1) that is essential at low frequencies. Including this fact we get the following expression for the threshold velocity:

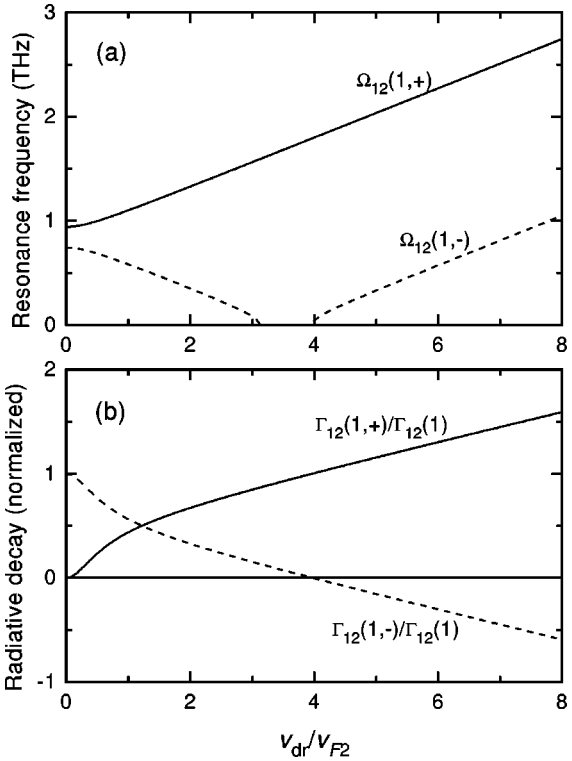

FIG. 8. (a) The resonance frequency $\Omega_{12}(m,\pm)$ and (b) the normalized radiative decay $\Gamma_{12}(m,\pm)/\Gamma_{12}(m)$ at $m=1$ as a function of the dimensionless drift velocity of the 2D electrons $U=v_{\rm dr}/v_{F2}$. Physical and geometrical parameters of the structure are the same as in Fig. 7.

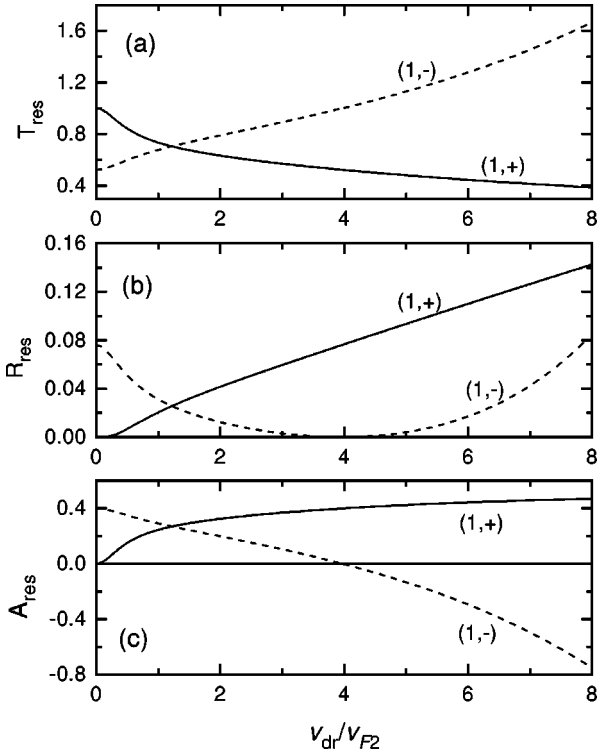

FIG. 9. The resonant values of (a) the transmission, (b) the reflection, and (c) the absorption coefficients for the modes $\Omega_{12}(m,\pm)$ at $m=1$ as a function of the dimensionless drift velocity of the 2D electrons $U=v_{\rm dr}/v_{F2}$. Physical and geometrical parameters of the structure are the same as in Fig. 7.

$$v_{\rm th}=\frac{\omega_{p2}(G_m)}{G_m}\left(1+\frac{\Delta_m}{2}X\right), \tag{55}$$

where the (positive) factor X is determined by the cubic equation

$$X^3+X^2=A\equiv\frac{8\gamma_2\Gamma_2(2\gamma_2+\Gamma_2)}{\Gamma_{12}(m)\omega_{p2}^2(G_m)\Delta_m^3}. \tag{56}$$

The threshold velocity thus consists of two contributions. The first one,

$$\frac{\omega_{p2}(G_m)}{G_m}=v_{F2}\sqrt{\frac{a}{2\pi a_B^\star|m|}}, \tag{57}$$

can be reduced by choosing the structures with a low 2D electron density n_2 and a small period a, and exploiting an excitation of higher 2D plasmon harmonics (here $a_B^\star$ is the effective Bohr radius). The second contribution due to the correction $\Delta_m X/2$ in Eq. (55) has a complicated dependence on the density n_2, the momentum relaxation rate γ_2, the mode index m, and the geometrical parameters of the structure. Qualitatively these dependencies can be understood if we note that the factor X equals $A^{1/3}$, if $A\gg1$, and $A^{1/2}$, if $A\ll1$, while the parameter A, in its turn, is proportional to

$$A\propto\gamma_2\left(1+\frac{2\gamma_2}{\Gamma_2}\right)\frac{a\,\exp(8G_mD)}{f^2J_1^2(\pi fm)} \tag{58}$$

(we consider the semielliptic density profile). Thus, the second contribution to the threshold velocity can be reduced if the parameter W/a satisfies the conditions (49), the distance between the 2DES and the grating is small as compared to the width of the grating strips, $D\ll W$, and the grating period a, as well as the momentum relaxation rate γ_2, are taken to be as small as possible. The f dependence of the normalized threshold velocity $v_{\rm th}/v_{F2}$ for several lowest modes $m=1,\ldots,4$, and for parameters of Fig. 3 ($n_{s2}=3\times10^{11}$ cm^{-2}, $\gamma_2=0.7\times10^{11}$ s^{-1}, $D=60$ nm) is shown in Fig. 11. The divergencies of $v_{\rm th}$ are related to zeros of the factor Δ_m.

The second effect which is not described by our single-resonance approximation is an anticrossing of modes with different m, which can be seen in Fig. 7 at $U\approx0.8$ and at $U\approx1.5$, where the relatively weak mode $(3,-)$ intersects the modes $(1,+)$ and $(1,-)$, respectively, as well as in Fig. 10 at $U\approx5.0$, where the mode $(3,-)$ (which has a positive slope with respect to $v_{\rm dr}$ at so large U) intersects the mode $(1,+)$ for a second time. The intersection points of modes $(m_1,-)$ and $(m_2,\pm)$ $(m_1>m_2)$ are determined by the relation $\Omega_{12}(m_1,-)=\Omega_{12}(m_2,\pm)$ [the modes $\Omega_{12}(m_1,+)$ and $\Omega_{12}(m_2,\pm)$ do not intersect at $m_1>m_2$], and the transmission, reflection, and absorption coefficients near the anticrossing can be found from Eqs. (31) and (32) in the limit $n_1\to\infty$ (metal grating) if we take into account only the terms with $m=m_1$ and $m=m_2$ in the sum in Eq. (32). The most interesting situation is realized at a large drift velocity, $v_{\rm dr}>\omega_{p2}(G_{m_1})/G_{m_1}$, when an *unstable* plasma mode $\Omega_{12}(m_1,-)$ intersects one of the stable plasma modes $\Omega_{12}(m_2,\pm)$ $(m_1>m_2)$. This occurs at the drift velocity

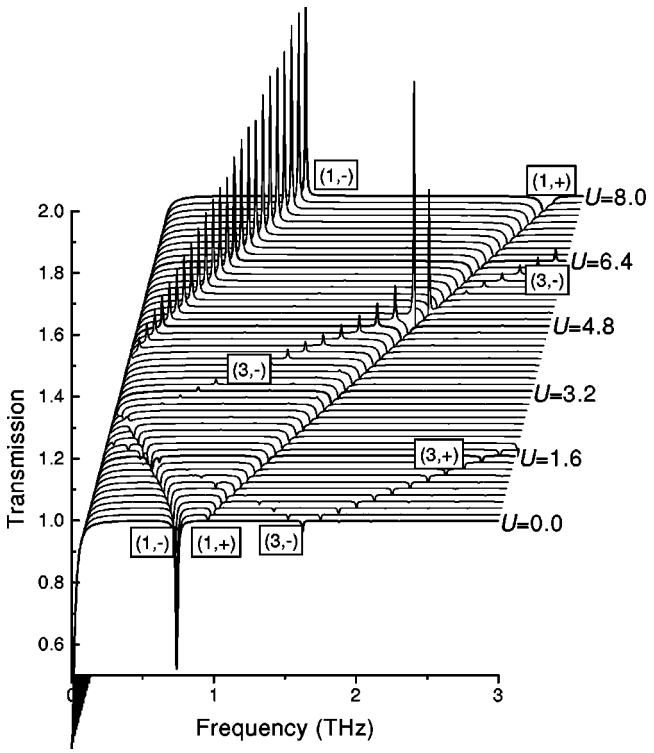

FIG. 10. The transmission coefficient of the structure metal grating–2DES at the frequency interval corresponding to the first ($m=1$) 2D plasmon harmonic in a wide range ($0 \leqslant U \leqslant 8$) of the dimensionless drift velocity $U=v_{\rm dr}/v_{F2}$. Physical and geometrical parameters of the structure are the same as in Fig. 3(a).

$$v_{\rm dr}^{(m_1,-),(m_2,\pm)} \approx \frac{\omega_{p2}(G_{m_1})+\omega_{p2}(G_{m_2})}{G_{m_1} \mp G_{m_2}}, \qquad (59)$$

and is accompanied by an enhancement of the amplification of waves, due to a resonant interaction of different plasma modes. In Fig. 10 one sees this effect at $U \approx 5.0$ [the intersection of modes $(3,-)$ and $(1,+)$]. A small resonance feature can be also seen at the intersection of modes $(3,-)$ and $(1,-)$ at $U \approx 2.6$ in the low-frequency range.

In vacuum devices one can easily achieve the drift velocity sufficient for the amplification of electromagnetic waves. In solid-state structures ''*metal* grating–2DES'' the discussed values of the threshold velocity are rather large. In order to make realistic estimations of achievable drift velocities in semiconductor heterostructures with the 2D electron gas we refer to the paper of Wirner *et al.*,[35] in which the dependence of the average drift velocity of 2D electrons as a function of the applied electric field has been experimentally investigated. The authors studied a $GaAs/Al_xGa_{1-x}As$ heterostructure with the density of 2D electrons of $n_2=6\times10^{10}$ cm^{-2} and the (low-field) mobility of $\mu_2=8\times10^5$ cm^2/V s. The corresponding Fermi velocity of 2D electrons is $v_{F2}=1.06\times10^7$ cm/s. The measured drift velocity of 2D electrons increases linearly with the applied electric field up to $E_0 \approx 50$ V/cm, sublinearly at larger fields and then saturates at $v_{\rm dr} \approx 1.8\times10^7$ cm/s when the field is increased up to $E_0 \approx 150$ V/cm. Based on the results of this experiment we will assume that the really achievable experimental values of the ratio $U=v_{\rm dr}/v_{F2}$ in $GaAs/Al_xGa_{1-x}As$ heterostructures with the low-density high-mobility 2D electron gas are restricted by the value of $U \approx 1.8$.

As seen from the above examples the threshold velocity is still well above the desired limit $U \approx 1.8$. It can be reduced, as compared to the numerical examples discussed above, by using smaller 2D electron gas density n_2, smaller grating period a, and larger 2D plasmon harmonics m. One of the problems in using the higher m in the structures ''*metal* grating–2DES'' is a small amplitude of 2D plasmon resonances with $m>1$ and their rapid decrease with increasing m, see Fig. 3. As we saw, however, in Sec. III C 2, the use of the *quantum-wire* grating allows one to increase the amplitudes of the higher 2D plasmon resonances by an order of magnitude [compare Figs. 6 and 3(c)], at the cost of the resonant interaction of 2D plasmons in the 2DES and the plasmons in wires. Using this effect, along with other methods discussed above, one can reduce the threshold velocity down to experimentally achievable values. An amplification of electromagnetic waves in the structure quantum-wire grating–2DES is considered in the next section.

B. Quantum-wire grating

In order to make a realistic estimation of the transmission coefficient of electromagnetic waves in the structure quantum-wire grating–2DES we do this for a hypothetic sample with parameters taken from published experimental papers. We assume that our sample is a $GaAs/Al_xGa_{1-x}As$ heterostructure ($m_1=m_2=0.067$) with the density of 2D electrons in the 2DES of $n_2=6\times10^{10}$ cm^{-2} (taken from Ref. 35). The low-field mobility in Ref. 35 was about $\mu_2 \approx 8\times10^5$ cm^2/V s, which corresponds to $\gamma_2 \approx 3.25\times10^{10}$ s^{-1}. In the high-field regime ($E_0 \approx 150$ V/cm) the mobility was by a factor of ~ 4 smaller, due to a heating of 2D electrons by a strong dc current. The dependence of the mobility on the dc current (or on the drift velocity) could be included into the theory through a phenomenological dependence of the momentum relaxation rate $\gamma_2(T_e)$ on the electron temperature. For our estimations we use, for simplicity, the drift velocity *independent* value $\gamma_2=1.3\times10^{11}$ s^{-1}, which corresponds to the mobility $\mu_2 \approx 2\times10^5$ cm^2/V s (roughly, this equals the ratio $v_{\rm dr}/E_0$ at $E_0 \approx 150$ V/cm in Ref. 35). Thus we assume the worst value of the momentum relaxation rate and take into account, effectively, the heating of 2D electrons by the strong dc current. For the grating we assume the same momentum relaxation rate of electrons, $\gamma_1=\gamma_2$.

Choosing the geometrical parameters of the structure we have assumed that modern experimental technique allows one to create periodic microstructures with lateral dimensions of order of 0.1 μm; see, e.g., Refs. 36, 37. The width of the grating strips is therefore taken to be $W=0.1$ μm, while the period $a=0.175$ μm is chosen in accordance with the rule (49) for $m=3$. The distance between the 2DES and the quantum-wire grating is assumed to be $D=20$ nm.

Figures 12 and 13 demonstrate the calculated transmission coefficient of the structure quantum-wire grating–2DES, near the intersection point of the unstable 2DES plasma mode $\Omega_{12}(3,-)$ and the grating plasmon. Two different values of the electron density in the grating, $n_1=n_2=6\times10^{10}$ cm^{-2} (Fig. 12) and $n_1=2n_2=1.2\times10^{11}$ cm^{-2} (Fig. 13), are used. Three important features seen in Figs. 12

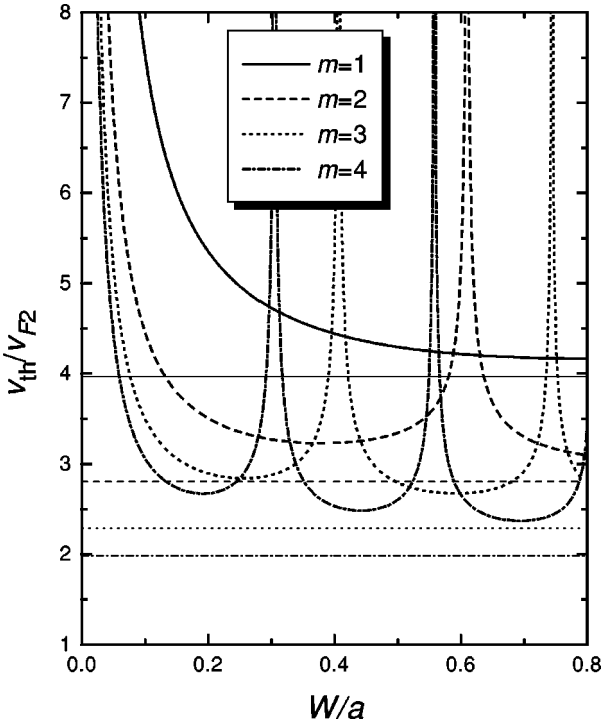

FIG. 11. Threshold velocity of the amplification as a function of the grating filling factor $f=W/a$ for several lowest mode numbers m, and at $n_{s2}=3\times10^{11}$ cm^{-2}, $\gamma_2=0.7\times10^{11}$ s^{-1}, $D=60$ nm. Thin lines show the first contribution to the threshold velocity (57).

and 13 should be mentioned. First, the resonant amplification of electromagnetic waves occurs at the drift velocities well below the experimentally achievable limit $U\approx1.8$. The value of $U\approx1.4$ (Fig. 12) corresponds to the drift velocity $v_{\rm dr}\approx1.4\times10^7$ cm/s and the dc current density $j_0\approx0.13$ A/cm

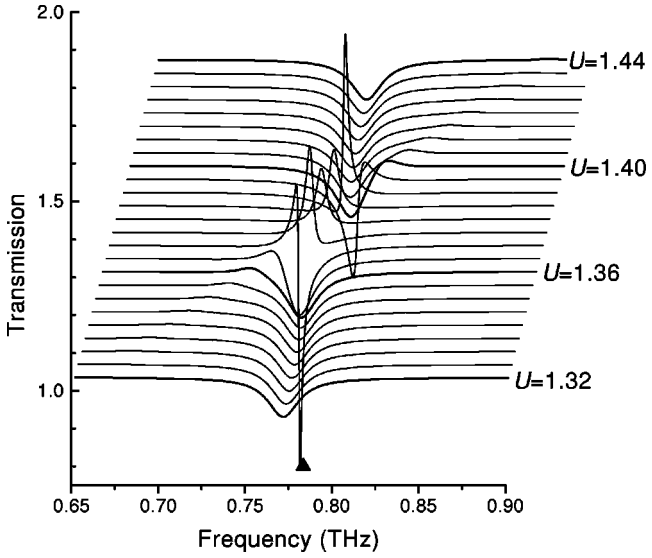

FIG. 12. Transmission coefficient of the structure quantum-wire grating–2DES for $n_1=n_2=6\times10^{10}$ cm^{-2}, $\gamma_1=\gamma_2=1.3\times10^{11}$ s^{-1}, $a=0.175$ μm, $W=0.1$ μm, and $D=20$ nm. The frequency and the drift velocity intervals correspond to an intersection of the grating plasmon and the $(3,-)$ 2D plasma mode. The black triangle at the bottom of the plot shows the position of the grating plasmon (36).

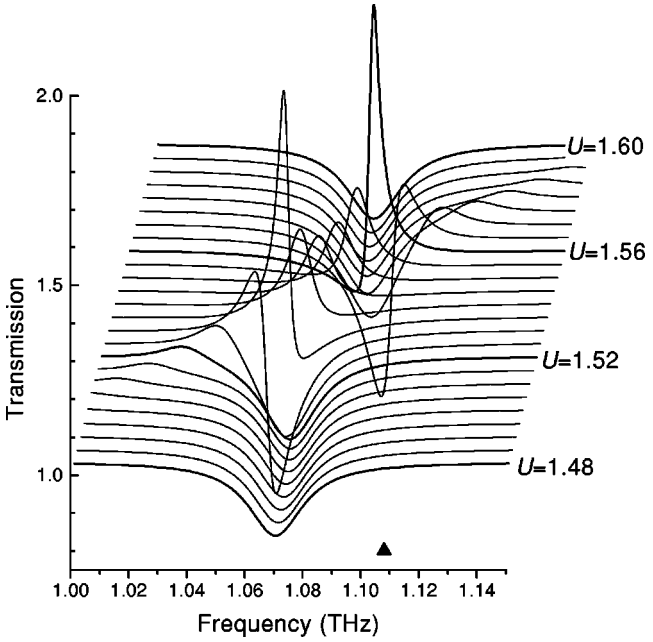

FIG. 13. The same as in Fig. 12, but for $n_1=2n_2=1.2\times10^{11}$ cm^{-2}.

in our example; in Ref. 35 this velocity has been achieved at $E_0\approx50$ V/cm. Second, the operating frequency of the amplifier lies in the vicinity of the intersection point of the grating plasmon $\tilde{\omega}_{p1}$ and the unstable mode $\Omega_{12}(m,-)$, at

$$v_{\rm dr}\approx\frac{\tilde{\omega}_{p1}+\omega_{p2}(G_m)\sqrt{1-\Delta_m/2}}{G_m},\quad \omega\approx\tilde{\omega}_{p1}. \tag{60}$$

It is varied by the dc current (the drift velocity) within about 10% with respect to $\omega\approx\tilde{\omega}_{p1}$ if the physical and geometrical parameters of the structure are kept constant (for instance, from ≈0.73 to ≈0.8 THz when U changes from 1.36 to 1.4 in Fig. 12, or from ≈1.03 to ≈1.13 THz when U changes from 1.52 to 1.58 in Fig. 13). The operating frequency can be also varied by changing the frequency $\tilde{\omega}_{p1}$ (compare Figs. 12 and 13), in quantum-wire structures tunable, e.g., by a gate voltage. Third, the absolute value of the amplification of waves near the resonances can be as great as several tens of percents, which is due exclusively to the resonant interaction of the 2D plasmons with the grating plasmon in the *quantum-wire* grating. For a comparison, in Fig. 14 we show the transmission coefficient of the structure metal grating–2DES for the same parameters of the 2DES, the same geometrical parameters, and in the same frequency and drift velocity intervals as in Fig. 13. A weak resonant feature that intersects the plot along the diagonal is the unstable mode $\Omega_{12}(3,-)$. As seen from Fig. 14, the amplification of waves in the metal grating structure is *several orders of magnitude* smaller than in the structure with the quantum wire grating (note the very large difference in the vertical axis scales in Figs. 13 and 14).

Thus an amplification of FIR radiation in structures with the quantum-wire grating can be obtained at realistic, experimentally achievable parameters.

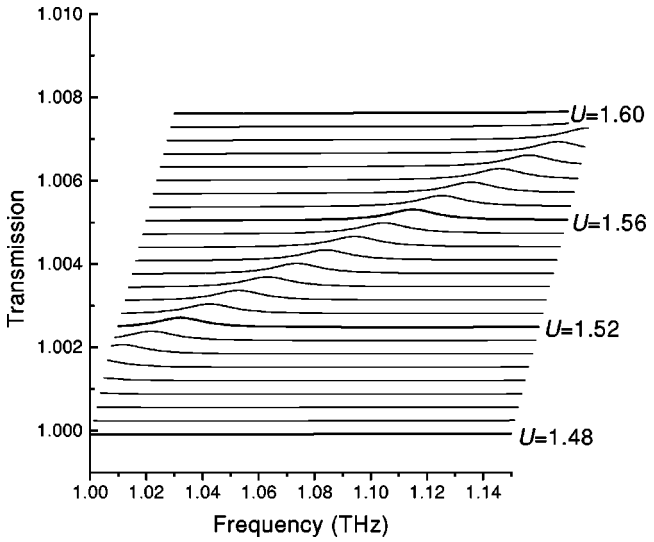

FIG. 14. The same as in Fig. 13, but for a metal grating with $n_{s1}=6\times10^{18}$ cm^{-2}, $\gamma_1=1.1\times10^{14}$ s^{-1}, and $m_1=1$. Note the large difference in the vertical axis scales in this figure and in Fig. 13.

V. EMISSION OF WAVES

In previous sections we have discussed an amplification of electromagnetic waves in the structure influenced by *both* the incident electromagnetic wave *and* the strong dc current (stimulated radiation). If the incident wave is absent, but the sample experiences a current flow, the system emits electromagnetic waves due to a disturbance of the thermal equilibrium (spontaneous radiation). This situation has been realized in experimental papers published so far.[8–13] In order to describe the emission spectrum using the formalism developed above one should include into the consideration the equilibrium blackbody radiation around the system, and take into account that the sample has a higher temperature (T_e) than the environment (T_0). Taking into account that the sample reflects and transmits the incident blackbody radiation with the intensity $I_{bb}(\omega,T_0)$, and emits the radiation with the intensity $A(\omega,v_{\rm dr})I_{bb}(\omega,T_e)$,[38] we obtain that the emitted radiation registered by an external device (filter) in the frequency interval between ω and $\omega+d\omega$ is given by[39]

$$E(\omega,v_{\rm dr})=A(\omega,v_{\rm dr})[I_{bb}(\omega,T_e)-I_{bb}(\omega,T_0)]. \quad (61)$$

Here $A(\omega,v_{\rm dr})$ is the absorption coefficient of the structure calculated in Sec. III, Eq. (25), and

$$I_{bb}(\omega,T_0)=\frac{\hbar\omega^3 d\omega}{4\pi c^2(e^{\hbar\omega/T_0}-1)}, \quad (62)$$

is the intensity of the blackbody radiation in the interval $(\omega,\omega+d\omega)$.

Figure 15 demonstrates the absorption (thin curves) and emission (thick curves) spectra of the structure metal grating–2DES under the conditions of the experiment of Ref. 13 ($n_2=5.4\times10^{11}$ cm^{-2}, $a=2$ μm and $a=3$ μm for two different samples, $W/a=0.6$ in both cases, $D=62$ nm, and the filter linewidth $\Delta f=85$ GHz). Plotting the figure we have assumed a steplike electron density profile in the grating (as the more relevant one in the case of the metal grating with wide strips), as well as the scattering rate $\gamma_2=5\times10^{11}$ s^{-1},

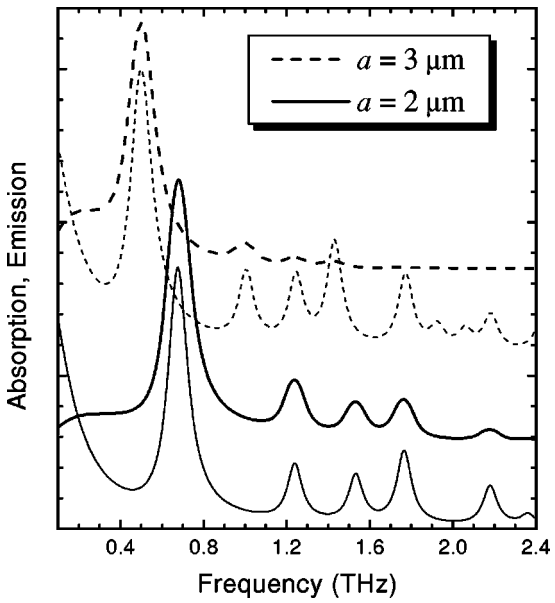

FIG. 15. The absorption (thin curves) and emission (thick curves) spectra of the structure metal grating–2DES for parameters taken from Ref. 13. The curves are vertically shifted for clarity, the absorption and emission are plotted in arbitrary units.

the environment temperature $T_0=4.2$ K, and $T_e=100$ K ($T_e=50$ K) for the sample with $a=2$ μm ($a=3$ μm). The whole behavior of the emission spectra qualitatively agrees with the measured ones, the position of peaks in Fig. 15 is in a good quantitative agreement with those measured in Ref. 13, see Table I.

It should be noted that the problem of the emission of light from the grating-coupled 2DES with a flowing current has been considered in Ref. 18. It has been solved in a complete analogy with the transmission problem. Such formulation of the emission problem is, however, not well defined and cannot give the emission spectrum (61) (the fact that the emission of light from the system is due to the blackbody radiation of a sample heated by the dc current has been ignored in Ref. 18). Indeed, when the transmission of light is calculated, one gets a set of equations for Fourier components of the total electric field (Sec. II or Ref. 17)

$$\sum_{\mathbf{G}'}\hat{M}_{\mathbf{G},\mathbf{G}'}E^{\rm tot}_{\mathbf{G}'}=E^{\rm ext}_{\mathbf{G}}, \quad (63)$$

where $\hat{M}_{\mathbf{G},\mathbf{G}'}$ is an infinite matrix over reciprocal lattice vectors. The spectrum of eigenmodes is determined by the equation $\det\hat{M}=0$, the total self-consistent electric field can be

TABLE I. Position of resonance peaks (THz) for two samples with the period $a=2$ μm and $a=3$ μm, measured in Ref. 13 and calculated in this work; see Fig. 15. For other parameters see the text.

	$m=1$	$m=2$	$m=3$
$a=2$ μm, expt.	0.69	1.3	
$a=2$ μm, theor.	0.68	1.24	
$a=3$ μm, expt.	0.47	0.9	1.26
$a=3$ μm, theor.	0.50	1.00	1.25

found from Eq. (63), if the matrix $\hat{M}$ is inverted.[17] The *transmission* problem is thus well defined.

In Ref. 18 the authors have derived a similar equation for the *emission* problem, when $v_{\rm dr}\neq 0$ and $\mathbf{E}^{\rm ext}=0$. In this case however, the right-hand side of Eq. (63) vanishes, and the drift velocity $v_{\rm dr}$ enters only the matrix $\hat{M}$. The spectrum of eigenmodes of the system (including unstable ones) can be calculated from the equation $\det \hat{M}=0$, but the induced radiated field $E^{\rm ind}_{\mathbf{G}=\mathbf{0}}$ cannot be found in this fashion, as the right-hand side of Eq. (63) is zero. Instead of the intensity of the emitted waves, Kempa *et al.*[18] calculated the ratio of the macroscopic (radiated) field $E^{\rm ind}_{\mathbf{G}=\mathbf{0}}$ to the microscopic (nonpropagating) field $E^{\rm ind}_{\mathbf{G}\neq\mathbf{0}}$. This ratio characterizes the grating as a coupler of the plasmon field to the propagating electromagnetic radiation, but is not an appropriate characteristic of the emission process, as it does not vanish, for instance, at $v_{\rm dr}=0$.

VI. SUMMARY

We have developed a general analytic theory of the transmission, reflection, absorption, and emission of electromagnetic waves in the structure ''2DES (with and without the flowing dc current)–grating coupler.'' We have demonstrated that an amplification, and hence a generation, of FIR radiation (the lasing effect) can be obtained in semiconductor microstructures with realistic experimental parameters. Summarizing our results we formulate the requirements that should be met in order to create a successfully working amplifier of FIR radiation based on the grating coupled 2DES with a flowing current.

(1) The density of electrons in the 2DES should be small. This requirement seems to be paradoxical, as the intensity of the transmission resonance at the vanishing drift velocity $v_{\rm dr}=0$ becomes very small when n_2 decreases. Nevertheless, at a large drift velocity the intensity of resonances becomes sufficiently large (Fig. 10), especially in the structures with a quantum wire grating (Figs. 12, 13), but the threshold velocity of amplification decreases with n_2, Eqs. (55), (57). Note that this requirement has not been satisfied in previous emission experiments (for instance, in Ref. 13 the 2D electron density was by an order of magnitude larger than the value that we have used in Figs. 12, 13). Note also that in vacuum devices the plasma frequency in the electron beam used to be very small ($G_1 v_{\rm dr}\gg\omega_p$).

(2) The mobility of 2D electrons should be sufficiently large; however, this requirement is not so crucial as others. As we have seen in Figs. 12 and 13, a considerable amplification of light could be achieved at a moderate mobility of $\mu_2\approx 2\times 10^5$ cm^2/V s.

(3) The most important requirement imposed on the grating is that it must be a *quantum-wire* grating, but not a commonly employed[8–13] metal one. It is the resonant interaction of plasma modes in the 2DES and in the grating that allows one to significantly increase the amplification of light when using the higher 2D plasmon harmonics, and hence to reduce the threshold velocity of amplification.

(4) The grating period should be as small as possible. This condition seems to be in some contradiction with another one, $a\gg D$, which follows from the requirement that the interaction of plasma modes in the 2DES and in the grating [described by the exponent $\exp(-G_m D)$, Eq. (48)] should be sufficiently large (for instance, in Ref. 13 the grating period was by an order of magnitude larger than the one we have used in Figs. 12, 13). Nevertheless, the inequality $D\ll a$ (more accurately, $D\ll W$, see below) should be considered as a condition for D, while the period should be taken to be small. As seen from Eqs. (57),(58), this leads to a reduction of the threshold velocity.

(5) The width of the quantum wires *must satisfy* the conditions (49) (or, $Wm/a=1,2,3,\ldots$, if the steplike profile seems to be more appropriate for a description of a particular system[40]). As seen from Fig. 11, a correct choice of the ratio W/a *is of particular importance*, especially when the higher 2D plasmon harmonics are used.

(6) The distance D between the 2DES and the grating should meet the condition $D\ll W$. This requirement follows from maximizing the exponent $\exp(-G_m D)$, Eq. (48), if we take into account that the ratio Wm/a is already fixed by the conditions (49).

(7) The operating frequency of amplifiers can be varied by the dc electric current flowing in the 2DES and/or by changing the electron density n_1 (more generally, the resonance frequency $\tilde{\omega}_{p1}$) in the quantum-wire grating.

We hope that these recommendations will be helpful in creating tunable FIR sources and lasers, based on electron semiconductor microstructures of low dimensionality.

ACKNOWLEDGMENTS

I thank N. Savostianova for many useful discussions and W. L. Schaich for sending me a copy of his unpublished work.[27]

APPENDIX A: SOLVING THE INTEGRAL EQUATION (15)

A general scheme of solving the integral equation (15) consists of the following. Let $O_n(x)$ be a set of orthogonal polynomials with respect to the weight function $\vartheta(x)$ that satisfy the condition

$$\int \frac{dx}{W}\,\vartheta(x)O_n(x)O_m(x)=\delta_{mn} \tag{A1}$$

[for the profile (37) $O_n(x)$ are the Chebyshev polynomials]. Substituting an expansion

$$E_x^{\rm tot}(x)=\sum_n C_n O_n(x) \tag{A2}$$

into Eq. (15), multiplying by $\vartheta(x)O_m(x)$, and integrating over dx we get an infinite set of equations

$$\sum_n (\delta_{mn}+L_{mn})C_n=E_0 W(\mathbf{0},\omega)\,\delta_{m0}, \tag{A3}$$

which can be solved approximately by truncating the matrix $\delta_{mn}+L_{mn}$ to a finite size $N\times N$. Here

$$L_{mn}=\frac{2\pi i f\langle\sigma_{1D}(\omega)\rangle}{\omega\epsilon}\sum_{\mathbf{G}} W(\mathbf{G},\omega)\kappa_G\beta_m(\mathbf{G})\beta_n^{\star}(\mathbf{G}), \tag{A4}$$

$\beta_m(\mathbf{G})=\langle\vartheta(x)O_m(x)e^{i\mathbf{G}\cdot\mathbf{r}}\rangle$, and the star means the complex conjugate. The approximation accepted in the main body of the paper corresponds to $N=1$. Physically, truncating the matrix to the 1×1 size we neglect effects related to an excitation of quadrupole and higher plasma eigenmodes[23] in the grating strips.

APPENDIX B: RESONANCE FREQUENCY IN AN ARRAY OF WIRES

Equation (36) gives an expression for a dipole excitation resonance frequency in an array of wires as a functional of the equilibrium electron density $\vartheta(x)$. It can be presented in different forms which clarify the role of the interwire interaction and the relation to the generalized Kohn theorem.[33]

1. Interwire interaction

In view of Eq. (45) one can write

$$\frac{\tilde{\omega}_{p1}^2}{\omega_{p1}^2}=\frac{\pi f W}{8}\sum_{G_m\neq 0}|G_m|\alpha(G_m). \tag{B1}$$

For a semielliptic density profile (37) the form factor $\alpha(G)$ is given by Eq. (38). Using the transformation

$$\sum_{G_m} F(G_m)=\int\frac{a\,dq}{2\pi}F(q)\sum_k e^{iqa_k}, \tag{B2}$$

where $a_k=ak$, we get

$$\frac{\tilde{\omega}_{p1}^2}{\omega_{p1}^2}=\int_{-\infty}^{\infty}\frac{dq}{|q|}J_1^2(qW/2)\sum_{k=-\infty}^{\infty}e^{iqak}. \tag{B3}$$

The term of the sum with $k=0$ is independent of the grating period a and gives, after the integration over dq, unity. It describes the contribution of a single wire. The corrections due to the interwire interaction are then written as

$$\frac{\tilde{\omega}_{p1}^2}{\omega_{p1}^2}=1+2\sum_{k=1}^{\infty}\int_0^{\infty}\frac{dx}{x}J_1^2(fx/2k)(e^{ix}+e^{-ix}). \tag{B4}$$

In the first (second) integral in Eq. (B4) we rotate the integration path by an angle $+\pi/2$ $(-\pi/2)$ to the upper (lower) complex half-plane. The function J_1 is transformed to I_1, and we have

$$\frac{\tilde{\omega}_{p1}^2}{\omega_{p1}^2}=1-4\sum_{k=1}^{\infty}\int_0^{\infty}\frac{dx}{x}e^{-x}I_1^2(fx/2k). \tag{B5}$$

The expansion (44) can now be easily obtained from Eq. (B5) at $f\ll 1$.

2. Relation to the generalized Kohn theorem

In many publications concerning the electromagnetic response of a confined system of electrons like quantum wires or quantum dots, the resonance frequencies are discussed in terms not of an equilibrium electron density, see Eq. (36), but of a confining potential. One can state a relation between these two approaches.

Let an array of wires be formed by an external confining potential (potential energy)

$$V_{\rm ext}(x)=\sum_k v_{\rm ext}(x-a_k). \tag{B6}$$

The total self-consistent potential $V_{\rm tot}(x)=V_{\rm ext}(x)+V_{\rm ind}(x)$ is given by the sum of external and induced potentials, where the induced potential $V_{\rm ind}(x)$ relates to the density (1) by the Poisson equation,

$$\Delta V_{\rm ind}(x,z)=-\frac{4\pi e^2 N_1(x)}{\epsilon}\delta(z). \tag{B7}$$

Equation (36) can be written as

$$\tilde{\omega}_{p1}^2=\frac{2\pi e^2}{m_1\epsilon W n_1}\sum_{m\neq 0}|G_m|N_{1,G_m}\int_{\rm cell}dx n_1(x)e^{iG_m x}, \tag{B8}$$

where the integral is taken over an elementary cell. Due to Eq. (B7) the Fourier component of the density $N_{1,G}$ is related to the Fourier component of the induced potential $V_{{\rm ind},G}=2\pi e^2 N_{1,G}/\epsilon|G|$, so that we can write Eq. (B8) for a single wire in the form

$$\omega_{p1}^2=-\frac{1}{m_1 n_1 W}\int dx n_1(x)\Delta_2 V_{\rm ind}(x), \tag{B9}$$

where Δ_2 is the two-dimensional Laplacian and the integral is expanded onto the whole axis. Replacing $V_{\rm ind}$ by the difference $V_{\rm tot}-V_{\rm ext}$, one sees that the contribution due to the total self-consistent potential vanishes, as $V_{\rm tot}$ is constant in points where electrons are. Thus, we have

$$\omega_{p1}^2=\frac{1}{m_1 n_1 W}\int dx n_1(x)\Delta_2 V_{\rm ext}(x). \tag{B10}$$

In a parabolic confining potential $V_{\rm ext}(x)=Kx^2/2$, and Eq. (B10) reproduces the statement of the generalized Kohn theorem,[33]

$$\omega_{p1}^2=K/m_1. \tag{B11}$$

*Electronic address: sam@mpipks-dresden.mpg.de

[1] S. J. Smith and E. M. Purcell, Phys. Rev. **92**, 1069 (1953).
[2] S. J. Allen, Jr., D. C. Tsui, and R. A. Logan, Phys. Rev. Lett. **38**, 980 (1977).
[3] T. N. Theis, J. P. Kotthaus, and P. J. Stiles, Solid State Commun. **24**, 273 (1977).
[4] D. C. Tsui, S. J. Allen, Jr., R. A. Logan, A. Kamgar, and S. N. Coppersmith, Surf. Sci. **73**, 419 (1978).

[5] T. N. Theis, J. P. Kotthaus, and P. J. Stiles, Solid State Commun. **26**, 603 (1978).
[6] T. N. Theis, Surf. Sci. **98**, 515 (1980).
[7] F. Stern, Phys. Rev. Lett. **18**, 546 (1967).
[8] D. C. Tsui, E. Gornik, and R. A. Logan, Solid State Commun. **35**, 875 (1980).
[9] E. Gornik, R. Schwarz, G. Lindemann, and D. C. Tsui, Surf. Sci. **98**, 493 (1980).
[10] R. A. Höpfel, E. Vass, and E. Gornik, Phys. Rev. Lett. **49**, 1667 (1982).
[11] R. Höpfel, G. Lindemann, E. Gornik, G. Stangl, A. C. Gossard, and W. Wiegmann, Surf. Sci. **113**, 118 (1982).
[12] N. Okisu, Y. Sambe, and T. Kobayashi, Appl. Phys. Lett. **48**, 776 (1986).
[13] K. Hirakawa, K. Yamanaka, M. Grayson, and D. C. Tsui, Appl. Phys. Lett. **67**, 2326 (1995).
[14] A. B. Mikhailovskii, *Theory of Plasma Instabilities* (Consultants Bureau, New York, 1974).
[15] M. V. Krasheninnikov and A. V. Chaplik, Zh. Eksp. Teor. Fiz. **79**, 555 (1980) [Sov. Phys. JETP **52**, 279 (1980)].
[16] M. V. Krasheninnikov and A. V. Chaplik, Zh. Eksp. Teor. Fiz. **88**, 129 (1985) [Sov. Phys. JETP **61**, 75 (1985)].
[17] L. Zheng, W. L. Schaich, and A. H. MacDonald, Phys. Rev. B **41**, 8493 (1990).
[18] K. Kempa, P. Bakshi, H. Xie, and W. L. Schaich, Phys. Rev. B **47**, 4532 (1993).
[19] S. A. Mikhailov, Phys. Rev. B **54**, 10 335 (1996).
[20] S. A. Mikhailov, Superlatt. Microstruct. **23**, 346 (1998).
[21] S. A. Mikhailov and N. A. Savostianova, Appl. Phys. Lett. **71**, 1308 (1997).
[22] An assumption on the infinitely thin grating strips implies that the thickness of strips is small as compared to the skin-layer thickness. This approximation holds for a quantum wire grating. For a metal grating this means that the grating strips should be transparent.
[23] I. L. Aleiner, Dongxiao Yue, and L. I. Glazman, Phys. Rev. B **51**, 13 467 (1995).
[24] S. J. Allen, Jr., H. L. Störmer, and J. C. M. Hwang, Phys. Rev. B **28**, 4875 (1983).
[25] L. D. Landau and E. M. Lifshitz, *Electrodynamics of Continuous Media* (Pergamon, Oxford, 1984).
[26] V. B. Shikin, T. Demel, and D. Heitmann, Zh. Eksp. Teor. Fiz. **96**, 1406 (1989) [Sov. Phys. JETP **69**, 797 (1989)].
[27] W. L. Schaich (unpublished).
[28] When a dc current flows in the system the absorption coefficient consists in two contributions. The first one in due to the dc current and is proportional to the real part of the static conductivity of the 2DES, the second contribution is due to the electromagnetic wave. Eq. (25) determines only the second contribution to the total absorption in the system.
[29] A. L. Fetter, Ann. Phys. (N.Y.) **81**, 367 (1973); **88**, 1 (1974).
[30] In Eq. (28) we have neglected the term describing the finite compressibility of the 2DES (see Ref. 29). This approximation holds if $a \gg a_B^\star$, where $a_B^\star$ is the effective Bohr radius.
[31] L. D. Landau and E. M. Lifshitz, *The Classical Theory of Fields* (Pergamon, New York, 1975).
[32] S. A. Mikhailov, Phys. Rev. B **54**, R14 293 (1996).
[33] L. Brey, N. F. Johnson, and B. I. Halperin, Phys. Rev. B **40**, 10 647 (1989).
[34] Alternatively, the mode $\Omega_{12}(m,-)$ can be classified at a large drift velocity, $G_m v_{\rm dr} > \omega_{p2}(G_m)$, as the mode $(-|m|,+)$.
[35] C. Wirner, C. Kiener, W. Boxleitner, M. Witzany, E. Gornik, P. Vogl, G. Böhm, and G. Weimann, Phys. Rev. Lett. **70**, 2609 (1993).
[36] D. Weiss, M. L. Roukes, A. Menschig, P. Grambow, K. von Klitzing, and G. Weimann, Phys. Rev. Lett. **66**, 2790 (1991).
[37] C. Dahl, B. Jusserand, and B. Etienne, Phys. Rev. B **51**, 17 211 (1995).
[38] L. D. Landau and E. M. Lifshitz, *Statistical Physics*, Part 1 (Pergamon, New York, 1970).
[39] In this estimation we ignore the angular dependence of the absorption coefficient, assuming that $A(\omega,\theta)=A(\omega,0)$, where θ is the angle between the normal to the plane of the 2DES and the direction of propagation of the blackbody radiation. Equations (61) and (62) are obtained by an integration over θ of the corresponding angular-dependent expressions.
[40] We believe that the semielliptic density profile is appropriate for quantum wires, while the steplike profile is more suitable for metal strips. In a general case, the factor $f^2\alpha(G_m)$ should have a maximum, see Eq. (48).